Magnitude and uncertainty of nitrous oxide emissions from North America based on bottom-up and top-down approaches: Informing future research and national inventories

Rongting Xu[1], Hanqin Tian[1], Naiqing Pan[1], Rona Louise Thompson[2], Josep G. Canadell[3], Eric A. Davidson[4], Cynthia Nevison[5], Wilfried Winiwarter[6], Hao Shi[1], Shufen Pan[1], Jinfeng Chang[7], Philippe Ciais[8], Shree R.S. Dangal[9], Akihiko Ito[10], Robert B. Jackson[11], Fortunat Joos[12], Ronny Lauerwald[13], Sebastian Lienert[14], Taylor Maavara[15], Dylan B. Millet[16], Peter A Raymond[17], Pierre Regnier[13], Francesco Nicola Tubiello[18], Nicolas Vuichard[19], Kelley C. Wells[16], Chris Wilson[20], Jia Yang[21], Yuanzhi Yao[1], Sönke Zaehle[22], and Feng Zhou[23]

[1]Auburn University
[2]Norwegian Institute for Air Research
[3]Global Carbon Project, CSIRO Oceans and Atmosphere
[4]University of Maryland Center for Environmental Science
[5]University of Colorado Boulder
[6]IIASA
[7]Zhejiang University
[8]Laboratory for Climate Sciences and the Environment (LSCE)
[9]Woods Hole Research Center
[10]National Institute for Environmental Studies
[11]Stanford University
[12]University of Bern
[13]Université Libre de Bruxelles
[14]University of Bern Physics Institute Climate and Environmental Physics & Oschger Centre for Climate Change Research
[15]School of the Environment, Yale University
[16]University of Minnesota
[17]Yale University
[18]FAO
[19]LSCE-IPSL
[20]Leeds University
[21]Mississippi State University
[22]Max Planck Institute for Biogeochemistry
[23]Peking University

November 28, 2022

Abstract

We synthesized N_2O emissions over North America using 17 bottom-up (BU) estimates from 1980-2016 and five top-down (TD) estimates from 1998-2016. The BU-based total emission shows a slight increase owing to U.S. agriculture, while no consistent trend is shown in TD estimates. During 2007-2016, North American N_2O emissions are estimated at 1.7 (1.0-3.0) Tg N yr^{-1} (BU) and 1.3 (0.9-1.5) Tg N yr^{-1} (TD). Anthropogenic emissions were twice larger than natural fluxes from soil and water. Direct agricultural and industrial activities accounted for 68% of total anthropogenic emissions, 71% of which was contributed by the U.S. Our estimates of U.S. agricultural emissions are comparable to the EPA greenhouse gas (GHG) inventory, which includes estimates from IPCC tier 1 (emission factor) and tier 3 (process-based modeling) approaches. Conversely, our estimated agricultural emissions for Canada and Mexico are twice as large as the respective national GHG inventories based on tier 1 approaches.

Hosted file

`xu et al. na n2o si.docx` available at https://authorea.com/users/557350/articles/606966-magnitude-and-uncertainty-of-nitrous-oxide-emissions-from-north-america-based-on-bottom-up-and-top-down-approaches-informing-future-research-and-national-inventories

Magnitude and uncertainty of nitrous oxide emissions from North America based on bottom-up and top-down approaches: Informing future research and national inventories

R. Xu[1,2], H. Tian[1], N. Pan[1], R. L. Thompson[3], J. G. Canadell[4], E. A. Davidson[5], C. Nevison[6], W. Winiwarter[7,8], H. Shi[1], S. Pan[1], J. Chang[9], P. Ciais[10], S. R. S. Dangal[11], A. Ito[12], R. B. Jackson[13], F. Joos[14], R. Lauerwald[15], S. Lienert[14], T. Maavara[16], D. B. Millet[17], P. A. Raymond[16], P. Regnier[18], F. N. Tubiello[19], N. Vuichard[10], K. C. Wells[17], C. Wilson[20,21], J. Yang[22], Y. Yao[1], S. Zaehle[23], F. Zhou[24]

[1]International Center for Climate and Global Change Research, School of Forestry and Wildlife Sciences, Auburn University, Auburn, AL, USA.
[2]Forest Ecosystems and Society, Oregon State University, Corvallis, OR, USA.
[3]Norsk Institutt for Luftforskning, NILU, Kjeller, Norway.
[4]Global Carbon Project, CSIRO Oceans and Atmosphere, Canberra, Australia.
[5]Appalachian Laboratory, University of Maryland Center for Environmental Science, Frostburg, MD, USA.
[6]University of Colorado Boulder/INSTAAR, Boulder, CO, USA.
[7]International Institute for Applied Systems Analysis, Laxenburg, Austria.
[8]Institute of Environmental Engineering, University of Zielona Góra, Zielona Góra, Poland.
[9]College of Environmental and Resource Sciences, Zhejiang University, Hangzhou, China.
[10]Laboratoire des Sciences du Climat et de l'Environnement, LSCE, CEA CNRS, UVSQ UPSACLAY, Gif sur Yvette, France.
[11]School of Natural Resources, University of Nebraska – Lincoln, NE, USA.
[12]Earth System Division, National Institute for Environmental Studies, Tsukuba, Japan.
[13]Department of Earth System Science, Woods Institute for the Environment, and Precourt Institute for Energy, Stanford University, Stanford, CA, USA.
[14]Climate and Environmental Physics, Physics Institute and Oeschger Centre for Climate Change Research, University of Bern, Bern, Switzerland.
[15]Université Paris-Saclay, INRAE, AgroParisTech, UMR ECOSYS, Thiverval-Grignon, France.
[16]Yale School of Forestry and Environmental Studies, New Haven, CT, USA.
[17]Department of Soil, Water, and Climate, University of Minnesota, MN, USA.
[18]Department Geoscience, Environment & Society-BGEOSYS, Université Libre de Bruxelles, Brussels, Belgium.
[19]Statistics Division, Food and Agriculture Organization of the United Nations, Via Terme di Caracalla, Rome, Italy.
[20]National Centre for Earth Observation, University of Leeds, Leeds, UK.
[21]Institute for Climate and Atmospheric Science, School of Earth and Environment, University of Leeds, Leeds, UK.
[22]Department of Forestry, Mississippi State University, Mississippi State, MS, USA.
[23]Max Planck Institute for Biogeochemistry, Jena, Germany.
[24]Sino-France Institute of Earth Systems Science, Laboratory for Earth Surface Processes, College of Urban and Environmental Sciences, Peking University, Beijing, China.

Corresponding author: Hanqin Tian (tianhan@auburn.edu)

Key Points:

- The total N_2O emissions over North American during 2007–2016 are estimated at 0.9–3.0 Tg N yr^{-1} using a combination of bottom-up and top-down approaches.
- North American anthropogenic N_2O emissions grew by ~0.2 Tg N during 1980–2016; U.S. agriculture was the largest cause of that growth.
- Modeled N_2O fluxes in this study reflect an IPCC tier 3 approach, and can improve GHG inventories that largely use tier 1 approaches.

Abstract

We synthesized N_2O emissions over North America using 17 bottom-up (BU) estimates from 1980–2016 and five top-down (TD) estimates from 1998–2016. The BU-based total emission shows a slight increase owing to U.S. agriculture, while no consistent trend is shown in TD estimates. During 2007–2016, North American N_2O emissions are estimated at 1.7 (1.0–3.0) Tg N yr^{-1} (BU) and 1.3 (0.9–1.5) Tg N yr^{-1} (TD). Anthropogenic emissions were twice larger than natural fluxes from soil and water. Direct agricultural and industrial activities accounted for 68% of total anthropogenic emissions, 71% of which was contributed by the U.S. Our estimates of U.S. agricultural emissions are comparable to the EPA greenhouse gas (GHG) inventory, which includes estimates from IPCC tier 1 (emission factor) and tier 3 (process-based modeling) approaches. Conversely, our estimated agricultural emissions for Canada and Mexico are twice as large as the respective national GHG inventories based on tier 1 approaches.

Plain Language Summary

Nitrous oxide (N_2O) is the third most important greenhouse gases (GHGs) after CO_2 and CH_4 causing global warming. Among world regions, North America (defined herein as U.S., Canada, and Mexico) is the second largest source of N_2O emissions globally, and previous source estimates for this region vary widely. This study aims to provide a comprehensive N_2O assessment over North America including all available estimates based on a number of approaches. We report total emissions, and emissions from four anthropogenic source sectors, over the past four decades. Agriculture and industry are two major N_2O sources in North America. Our results show a minor increase in the total N_2O emission due to agricultural trends in the U.S. Our bottom-up estimate of U.S. agricultural N_2O emissions are close to those in the EPA national GHG inventory that includes both empirical and modeled results. The high consistency suggests the need to take process-based modeling results into account for future national GHG inventories.

1 Introduction

Atmospheric nitrous oxide (N_2O), the third most-important greenhouse gas (GHG) and a key stratospheric ozone-depleting substance, has increased by 21% globally since 1750 due to anthropogenic activities (Ciais et al., 2014; Prinn et al., 2018). North America is the second-largest contributor to total global anthropogenic N_2O emissions (Tian et al., 2020a)—a region that consumed 16% of the world's synthetic nitrogen (N) fertilizer (Lu & Tian, 2017; FAO, 2021), produced 9% of the world's animal manure (Zhang et al., 2017; FAO, 2021), and received 16% of the world's atmospheric N deposition from industrial and agricultural activities (Eyring et al., 2013). An emission hot spot has also been observed in the Midwestern Corn Belt, one of the most intensively managed agricultural areas in the world and which accounted for 30% of total North American emissions during the period 2008–2014 (Nevison et al., 2018).

Bottom-up (BU; i.e., inventories and models) and top-down (TD; i.e., atmospheric inversions) approaches represent the two primary methods for estimating global, regional and country level emissions (Miller et al., 2012; Nevison et al., 2018; Saikawa et al., 2014; Shang et

al., 2019; Stehfest & Bouwman, 2006; Tian et al., 2016; Tian et al., 2020a; Wilson et al., 2014; X. Xu et al., 2012); a number of studies have estimated N_2O emissions from North America based on both approaches. Yet considerable uncertainty remains in estimates of total and sectorial emissions. For example, it is a long-standing debate whether BU emission inventories may underestimate N_2O emission over North America, especially in the Midwestern Corn Belt (Chen et al., 2016; Del Grosso et al., 2010; T. Griffis et al., 2013; Kort et al., 2008; Miller et al., 2012; Nevison et al., 2018). Moreover, current uncertainty in estimates of North American N_2O emissions could be reduced by reconciling the TD inversions with BU calculations.

The present study synthesized available N_2O emissions over North America [defined here as the region comprising the United States (U.S.), Canada, and Mexico] using 17 BU (emission inventories, spatial extrapolation of field flux measurements, nutrient budget modeling, and terrestrial biosphere models) and five TD estimates for the period 1980–2016 (Figure S1). Data sources for all estimates are consistent with Tian et al. (2020a). We examined estimates of N_2O emissions and the associated uncertainties for both approaches. In addition, national GHG emissions inventories developed by the U.S. (based on both Tier 1 and Tier 3 methods), by Canada and Mexico (Tier 1)) were used to compare against the BU estimates in this study of national total and sectorial N_2O emissions relative to the period 1990-2016.

2 Materials and Methods

2.1 Data Sources

2.1.1 Bottom-up Estimates

We collected N_2O emissions from 17 BU estimates. National N_2O emissions from models and inventories include: six terrestrial biosphere models for natural and cropland soils with consideration of multiple environmental factors [Global N_2O Model Inter-comparison Project (NMIP, Tian et al. (2019)]; three Dynamic Land Ecosystem Model (DLEM)-only simulations [i.e, for pastures (Dangal et al., 2019), rivers and reservoirs (Yao et al., 2020), and biomass burning]; two mechanistic stochastic model simulations for the river-reservoir-estuary continuum (Maavara et al., 2019) and lakes (Lauerwald et al., 2019); three national GHG emissions inventories [EDGAR v4.3.2, Janssens-Maenhout et al. (2019); FAOSTAT, Tubiello (2019); GAINS, Winiwarter et al. (2018)]; one fire emissions database for biomass burning [GFED4s, Van Der Werf et al. (2017)]; one statistical model for cropland soils [SRNM, Wang et al. (2019)]; and one estimate of aquaculture emissions calculated based on quantified N flows from a nutrient budget model (Bouwman et al., 2013). Six terrestrial biosphere models participated in NMIP provided N_2O emissions from natural and agricultural soils. All participating models were driven by consistent input datasets (i.e., climate, atmospheric CO_2 concentration, land cover change, atmospheric N deposition, mineral N fertilization, and manure N application) at the spatial resolution of 0.5° globally and covered the 1861–2016 period (Tian et al., 2019). Model-based estimates of national N flows (i.e., fish feed intake, fish harvest, and waste) in freshwater and marine aquaculture were obtained from Beusen et al. (2016) and Bouwman et al. (2011, 2013). We then calculated aquaculture N_2O emissions by considering 1.8% loss of N waste in aquaculture, the same EF used in MacLeod et al. (2019). EF uncertainties of aquaculture N_2O range from 0.5% (IPCC, 2006)) to 5% (Williams & Crutzen,

2010). A detailed description of each BU method was documented in the Supplementary Information of Tian et al. (2020a).

Anthropogenic N_2O emissions have been reported annually by Annex I Parties to the United Nations Framework Convention on Climate Change (UNFCCC) for nearly thirty years, currently covering the period 1990-2019. More recently, also the other signatories to the UNFCCC have been requested to provide information on their national greenhouse gas inventories as a Biannual Update Report, with sufficient detail and transparency to track progress towards their nationally determined contributions. In this study, we obtained time-series anthropogenic N_2O emissions from the most recent UNFCCC reporting that was submitted by the U.S. (Annex I Party; EPA GHG inventory, https://unfccc.int/documents/272415), Canada (Annex I Party; Canadian GHG inventory, https://unfccc.int/documents/271493), and Mexico (Non-Annex I Party; Mexican GHG inventory, https://unfccc.int/documents/199243) to compare with our estimates.

2.1.2 Top-down Estimates

We include five estimates from four independent atmospheric inversion frameworks for the 1998– 2016 period [INVICAT, Wilson et al. (2014); PyVAR-CAMS, Thompson et al. (2014); MIROC4-ACTM, Patra et al. (2018); and GEOSChem, Wells et al. (2015)], all of which used the Bayesian inversion method. Here, two versions of PyVAR-CAMS were run to determine the sensitivity of results to the prior estimate of ocean fluxes. These runs using high and low ocean priors are denoted as PyVAR-CAMS-1 and PyVAR-CAMS-2, respectively. For analyzing TD estimates over North America, we interpolated the coarser resolution results into $0.5° \times 0.5°$ over all land areas in the four frameworks (see Table S19 in Tian et al. (2020a)). A detailed description of each TD approach was documented in Supplementary Information of Tian et al. (2020a).

2.2 Data Synthesis

BU approaches give N_2O emissions estimates for five source categories, while TD approaches only provide total gridded emissions. BU estimates consist of N_2O emissions from natural sources (i.e., 'Natural soil baseline' and natural emissions from inland water and estuaries), and from 12 anthropogenic sub-categories that were combined and further re-classified into four categories (Table 1, Figure S1): i) 'Perturbed fluxes from climate/CO_2/land cover change' covering the CO_2 effect, climate effect, post-deforestation pulse effect, and long-term effect of reduced mature forest area, ii) 'Direct emissions of N additions in the agricultural sector (Agriculture)' covering direct application of synthetic N fertilizers and manure (direct soil emissions), manure left on pasture, manure management, and aquaculture, iii) 'Indirect emissions from anthropogenic N additions' covering atmospheric N deposition (NDEP) on land, and effects of anthropogenic loads of reactive N in inland waters and estuaries, and iv) 'Other direct anthropogenic sources' covering fossil fuel and industry, waste and waste water, and biomass burning. Here, 'Natural soil baseline' emissions reflect a situation without considering land use change (e.g., deforestation) and without considering anthropogenic N additions and indirect anthropogenic effects of environmental changes (i.e., climate, elevated CO_2, and atmospheric N deposition). The four categories are aligned with the emission categories in the UNFCCC reporting and IPCC 2006 methodologies [see Table S14 in Tian et al. (2020a)].

3 Results and Discussion

3.1 BU and TD Estimates of Total N_2O Emissions During 1980–2016

BU and TD approaches diverge in the magnitude and trend of the total emission over North America during 1980–2016 (Figure 1). In addition, larger uncertainties are derived for BU estimates than for TD estimates, likely because the BU uncertainty is the sum of ranges (minimum and maximum estimates) from 17 BU estimates with considerable contributions from natural soils, agriculture, and the effects of climate and CO_2 (Table 1). During 1998–2016, the BU estimate was 390 (70–1350) Gg N yr^{-1} higher than the TD estimate, but the latter implied a larger interannual variability (150 Gg N yr^{-1}). The BU estimate demonstrated a steady increase at a rate of 5±2 Gg N yr^{-1} per year (95% confidence interval; $P<0.05$) during 1980–2016, while the TD estimate decreased sharply between 1998 and 2005 and then started to increase again during 2006–2016, resulting in no significant overall trend. In the recent decade (2007–2016), North American total N_2O emissions were 1,680 (950–3,040) Gg N yr^{-1} (BU) and 1,260 (910–1,510) Gg N yr^{-1} (TD) (Table 1). BU estimates for the U.S., Canada, and Mexico were 1,150 (690–2110) Gg N yr^{-1}, 270 (120–520) Gg N yr^{-1}, and 260 (60–450) Gg N yr^{-1}, respectively.

Table 1. N_2O emission sources (expressed in Gg N yr^{-1}) over North America (i.e., U.S., Canada, and Mexico) during 2007–2016. All numbers are rounded to the nearest multiple of 10 for sources >10 and nearest whole number for sources <10.

2007-2016		USA			Canada			Mexico			North America		
Anthropogenic sources		**mean**	**min**	**max**	**mean**	**min**	**max**	**mean**	**min**	**max**	**mean**	**min**	**max**
Direct emissions of N additions in the agricultural sector (Agriculture)	Direct soil emissions	300	180	620	40	20	60	30	10	70	370	220	730
	Manure left on pasture	70	70	70	10	10	10	30	20	30	100	100	110
	Manure management	20	10	20	0	0	10	10	0	10	30	10	30
	Aquaculture	N/A	N/A	N/A	N/A	N/A	N/A	N/A	N/A	N/A	1	0	2
	sub-total	390	260	710	50	30	80	70	30	110	500	330	870
Other direct anthropogenic sources	Fossil fuel and industry	160	150	170	20	20	20	90	10	160	260	180	350
	Waste and waste water	20	20	20	0	0	0	10	0	10	30	30	30
	Biomass burning	20	10	40	30	10	60	0	0	0	60	30	100
	sub-total	200	180	230	50	30	80	100	10	170	350	240	480
Indirect emissions from anthropogenic N additions	Inland waters, estuaries, coastal zones	40	10	60	20	10	30	10	1	10	70	50	80
	Atmospheric N deposition on land	80	30	240	10	10	30	10	10	20	110	50	280
	sub-total	120	40	300	30	20	60	20	10	30	180	100	360
Perturbed fluxes from climate/CO2/land cover change	Climate & CO_2 effect	40	-80	220	10	-30	50	-10	-20	3	40	-120	280
	Post-deforestation pulse effect	120	120	120	10	10	10	10	10	20	140	140	150
	Long-term effect of reduced mature forest area	-50	-50	-50	-10	-10	-10	-20	-20	-30	-80	-80	-80
	sub-total	110	-10	290	10	-30	50	-20	-30	-10	100	-60	350
Anthropogenic total		820	470	1,530	140	50	270	170	20	300	1,130	610	2,060
Natural fluxes													
Natural soils baseline		320	210	560	100	40	220	90	40	150	510	300	930
Natural (Inland waters, estuaries, coastal zones)		10	10	20	30	30	30	1	1	2	40	40	50
Natural total		330	220	580	130	70	250	90	40	150	550	340	980
Bottom-up total source		**1,150**	**690**	**2,110**	**270**	**120**	**520**	**260**	**60**	**450**	**1,680**	**950**	**3,040**
Top-down total source											**1,260**	**910**	**1,510**

Based on BU estimates, U.S. anthropogenic N_2O emissions were 7% higher in 2007–2016 than in the 1980s, primarily because of a 27% increase in direct soil agricultural emissions (Figure 2). In Mexico, total anthropogenic emissions are estimated to have increased by 114%, due to a large yet quite uncertain contribution from industrial emissions over the most recent decades, according to EDGAR v4.3.2 data (Figure 2; Table S1). By contrast, anthropogenic emissions in Canada were relatively stable, with a slight increase in agricultural emissions offset by a reduction in emissions from industrial activities. Natural soil emissions were relatively constant in the three countries.

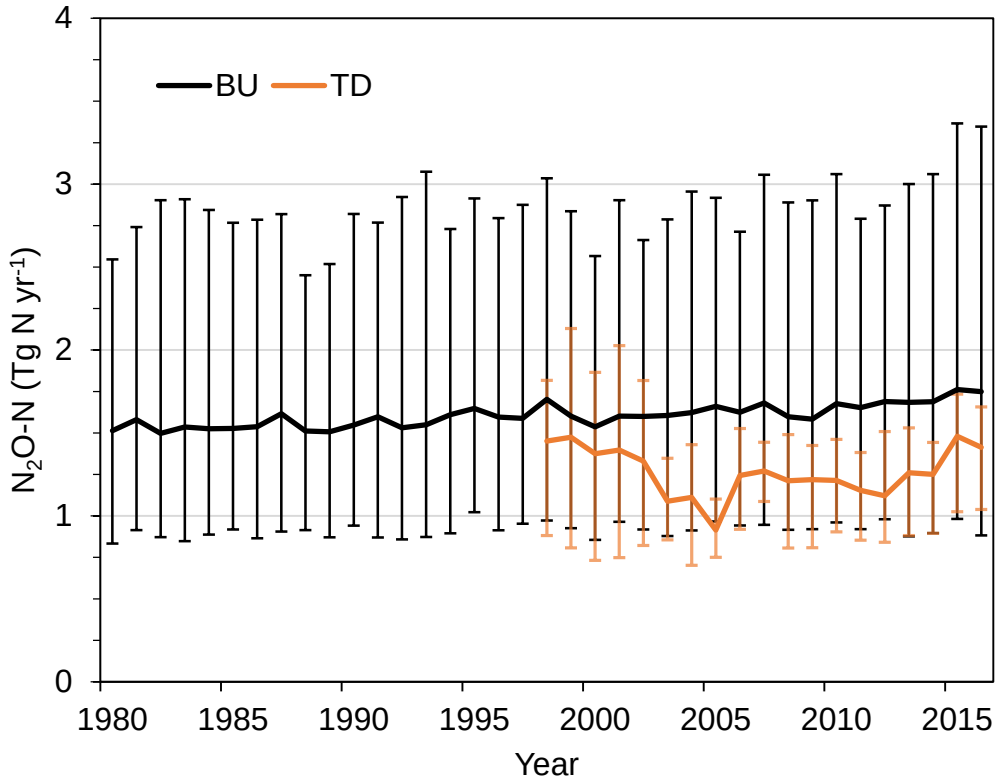

Figure 1. Comparison of annual total N_2O emissions from North America estimated by BU approaches during 1980–2016 and TD approaches during 1998–2016. Error bars indicate the spread between the minimum and the maximum values.

3.2 BU Estimates of N_2O Emissions Over 2007–2016

Two-thirds of total North American N_2O emissions during 2007–2016 were linked to anthropogenic sources, which averaged 1,120 Gg N yr^{-1} versus 550 Gg N yr^{-1} from natural sources (Table 1). Among the anthropogenic emissions, agriculture (45%) was the largest contributor, heavily dominated by direct soil emissions from synthetic N fertilizer and manure application, followed by emissions associated with manure left on pasture in the U.S., reflecting increased agricultural N inputs (Lu & Tian, 2017; Xu et al., 2019; FAO, 2021). Aquaculture played a negligible role in North American N_2O emissions. Direct soil emissions were the largest agricultural source in all three countries, with fluxes in both Canada and Mexico about an order of magnitude lower than those in the U.S (Figures S2-S4). Livestock manure-induced emissions (i.e., manure left on pasture and manure management) were five times lower than direct soil

emissions in the U.S. and Canada, however, this source was comparable to direct agricultural soil emissions in Mexico, where there has been a continuous increase in livestock numbers and manure production since 1980 (FAO, 2020; Zhang et al., 2017).

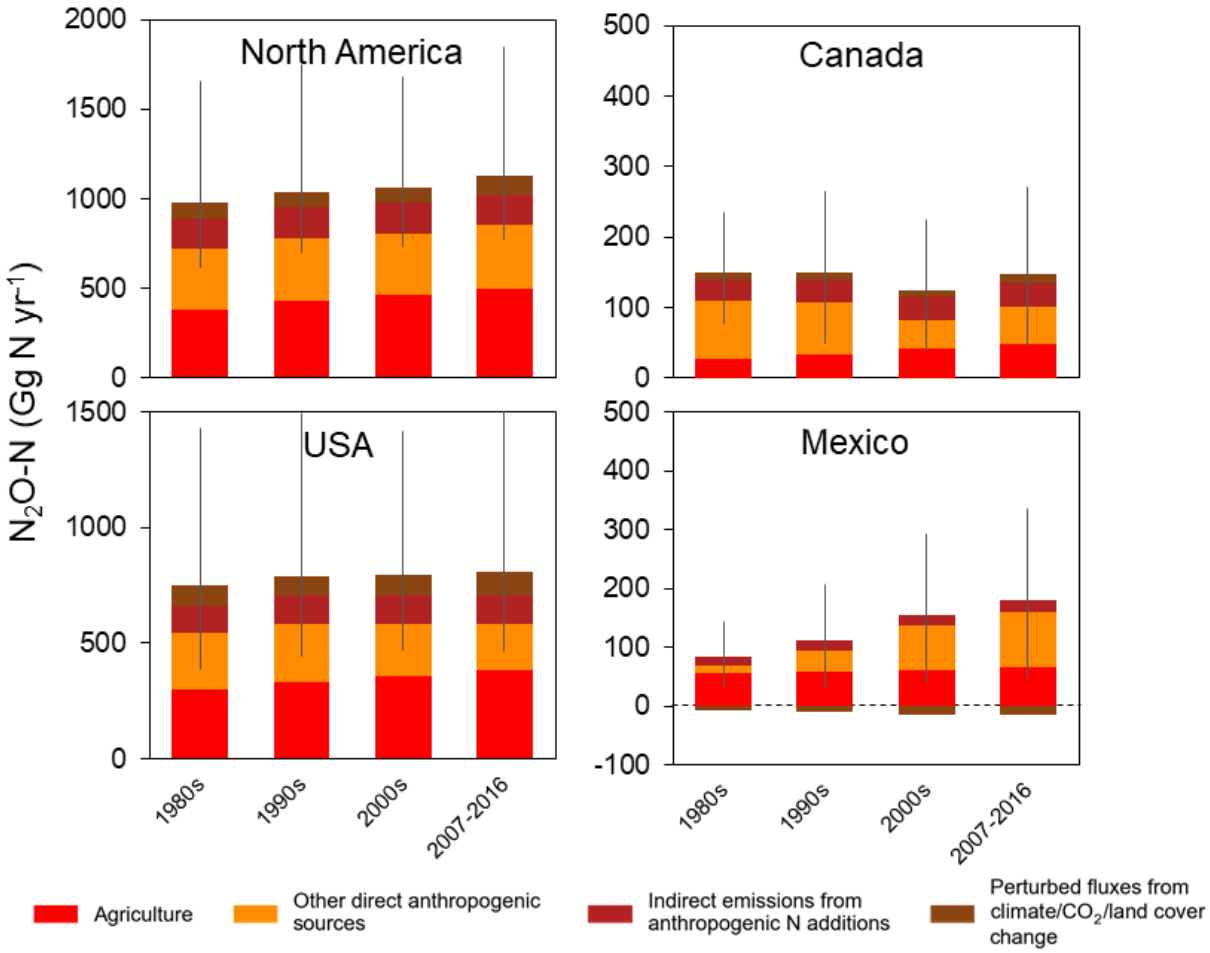

Figure 2. Ensembles of anthropogenic N_2O emissions over North America in the 1980s, 1990s, 2000s, and 2007–2016 based on BU approaches. Error bars indicate the spread between the minimum and the maximum values of the total flux.

Other direct anthropogenic sources (31%) made up the second-largest contribution to total continental emissions, and were primarily associated with emissions from fossil fuel and industry in the U.S. and Mexico during 2007–2016 (Table 1). Biomass burning was another important source of N_2O but diverged across these three countries; such emissions in Canada were twice and five times as high as in the U.S. and Mexico, respectively, between 2007 and 2016. Waste and waste water contributed least, with the largest share from the U.S. owing to its large population (FAO, 2021). Indirect emissions due to anthropogenic N additions from NDEP (110 Gg N yr^{-1}) and mostly due to agricultural N leaching to inland and coastal waters (70 Gg N yr^{-1}) accounted for 15% of North American anthropogenic emissions during 2007–2016. Among the three North American countries, the U.S. had the most intensive agricultural activities and thus its indirect emissions were much higher than those from Canada and Mexico (Table 1). Agricultural activity in the U.S., especially the Midwest, was the major driver for high indirect

emissions from NDEP (primarily ammonium) and leaching/runoff (primarily nitrate) from synthetic N fertilizer and livestock manure (Chen et al., 2016; Du et al., 2016; Tian et al., 2020b). We observed a considerable decline in NDEP-induced N_2O emissions from U.S. and Canadian industrial activities due to enforcement of the amendments to the Clean Air Act in 1995, though this decline was overwhelmed by the effect of indirect emissions caused by N losses from agriculture (Figures S2-S3). In contrast, Mexico showed a continuous increase in indirect emissions from NDEP due to increases in both agricultural and industrial activities (Figure S4).

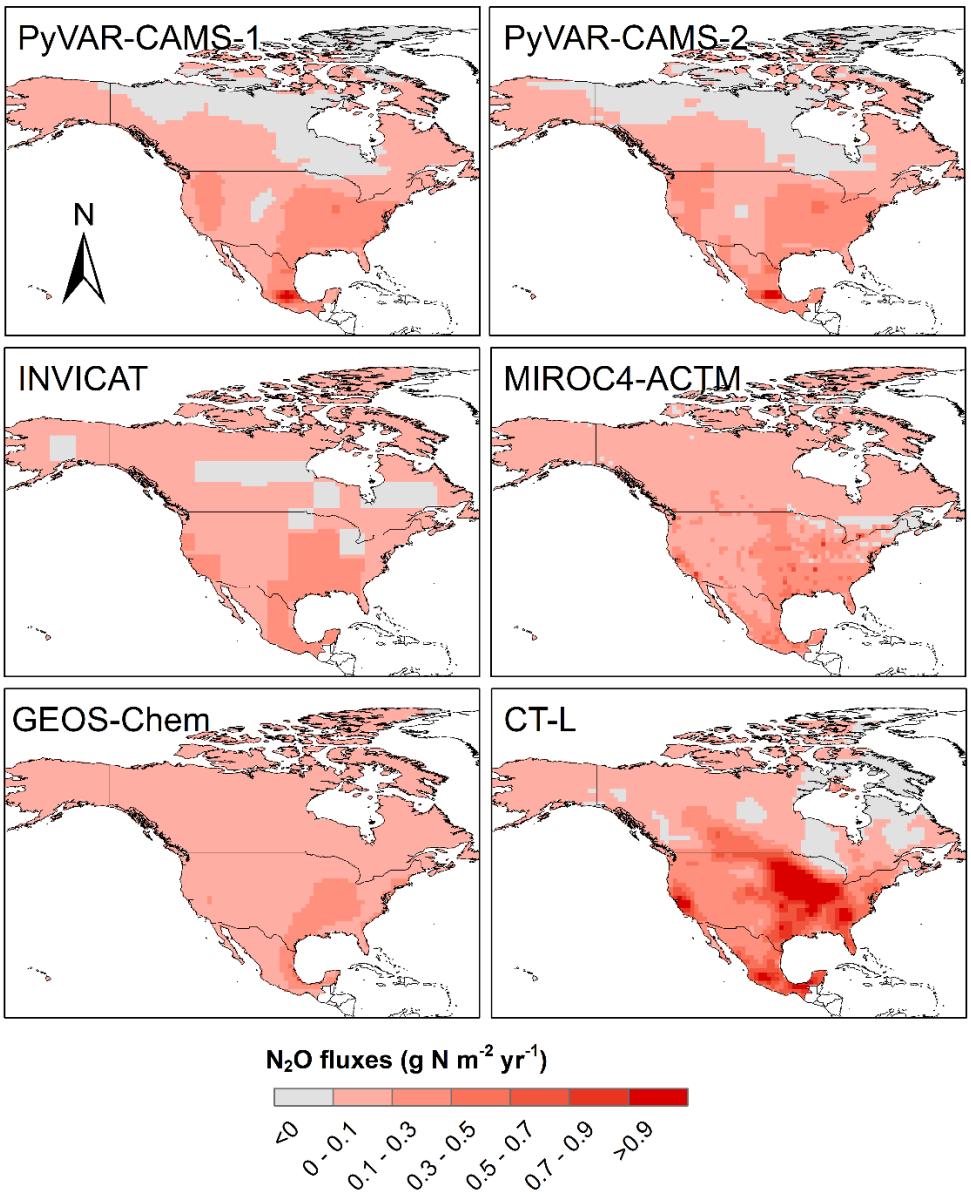

Figure 3. Comparison of our total N_2O emissions by global inversion models with the estimate by CT-L (Nevison et al., 2018) during 2008–2013. Global inversion models include PyVAR-CAMS, INVICAT, MIROC4-ACTM, and GEOS-Chem.

Perturbed fluxes caused by climate/CO_2/land cover change contributed the least (9%) to total anthropogenic emissions over North America according to model simulations. The effects of climate and CO_2 accelerated soil N_2O emissions with regional climate change. This has offset the reduction due to elevated CO_2 concentrations that enhance plant growth and associated N uptake and in turn decrease soil N_2O emissions (Tian et al., 2019; Zaehle et al., 2011). The decrease in perturbed fluxes of soil N_2O emissions over North America was only 80 Gg N yr^{-1} (only 7% of the global reduction), because temperate forest soils generally have lower emissions than tropical forest soils and because the area of converted lands was much smaller than in the tropics (e.g., Amazon) between 2007 and 2016 (Hurtt et al., 2011). This decrease can be balanced by the temporary rise of soil N_2O emission after deforestation (post-deforestation pulse effect) plus background emissions from converted croplands or pastures (McDaniel et al., 2019; Meurer et al., 2016; van Lent et al., 2015; Verchot et al., 1999). In particular, within the U.S. the decrease in soil N_2O emissions has been fully offset by the post-deforestation pulse effect, resulting in a positive increment of 60 Gg N yr^{-1}; however, this was not the case in Mexico where only half of the emission decrease was counterbalanced in this way (Table 1).

3.3 Comparison and Uncertainty

Previous estimates of total N_2O emissions over North America from TD approaches diverge in terms of magnitude and in terms of inter- and intra-annual variations. Saikawa et al. (2014) provided an estimate of 1.2±0.2 Tg N yr^{-1} over North America between 2004 and 2008 using data from six measurement networks with extensive spatial coverage to constrain the global budget. Their estimates are in line with our ensemble [1.2 (0.9–1.4) Tg N yr^{-1}] based on five TD estimates during the same period. Employing the posterior flux from the global atmospheric N_2O inversion of Saikawa et al. (2014) as the standard prior, Nevison et al. (2018) estimated North American N_2O emissions of 1.6±0.3 Tg N yr^{-1} over 2008–2014 using the CarbonTracker-Lagrange (CT-L) regional inversion framework. The Midwestern Corn/Soybean Belt – an emission hot spot - accounted for 30% of total emissions from North America (Nevison et al., 2018), but this hot spot was weaker in the global inversions (Figure 3). In addition, Midwestern Corn/Soybean N_2O emissions are elevated in spring and early summer owing to intensive N fertilizer applications and freeze-thaw dynamics (Nevison et al., 2018). Although the global and regional inversions had highest spring emissions, their amounts were obviously divergent (Figure S5). For example, PYVAR-CAMS and MIROC4-ACTM showed close spring N_2O emissions to the CT-L regional inversion, while INVICAT and GEOS-Chem showed much lower emissions compared to CT-L. A number of factors may contribute to the large discrepancy in estimated N_2O emissions between global inversion models and regional inversion (Nevison et al. 2018). First, the latter study used a substantially larger set of North American measurements, particularly NOAA aircraft data over the Midwest, especially with respect to MIROC4-ACTM (Tables S2 & S3). Second, the soil prior used in three global inversion models (PYVAR-CAMS, INVICAT, and GEOS-Chem) were from the model OCN-v.1.1 that showed a much lower spring N_2O emissions from agricultural soils (Figures S6 & S7) and thus tended to shift the soil maximum away from spring and the Midwest. Third, the time frame of the global inversions (1995–2016) might dilute the impact of Midwestern sites like West Branch Iowa (WBI), which came online mid-2007, whereas the CT-L regional inversion focused on a subset of that period (2008–2015) that emphasized the impact of WBI (Table S3). Finally, the global inversions used much coarser resolution models [e.g., INVICAT (5.625°; at the scale of ~620km)] compared to CT-L at the spatial resolution of 1° (~111km) (Table S4). Thus, global models cannot reproduce

as well the small variations in atmospheric concentration and distribute the emissions more diffusely in the Midwest Corn/Soybean belt extending from 36°N to 47°N (~1220km) and 102° to 80°W (~2440km).

High N_2O emission in the Midwestern Corn/Soybean Belt was also reported by all six BU terrestrial biosphere models but to different degrees (Figure S7): DLEM and VISIT show much higher emissions than the other four models (LPX-Bern, OCN, ORCHIDEE, and ORCHIDEE-CNP). Seasonal N_2O emissions from the BU models were highest in summer and autumn (Figure S6), which differs from the regional (Nevison et al. 2018) and global inversions. The lower spring N_2O emissions estimated by BU models are probably associated with the widely varied timing of N fertilizer application in each model and the omission of freeze-thaw and wet-dry dynamics in some of model structure configurations.

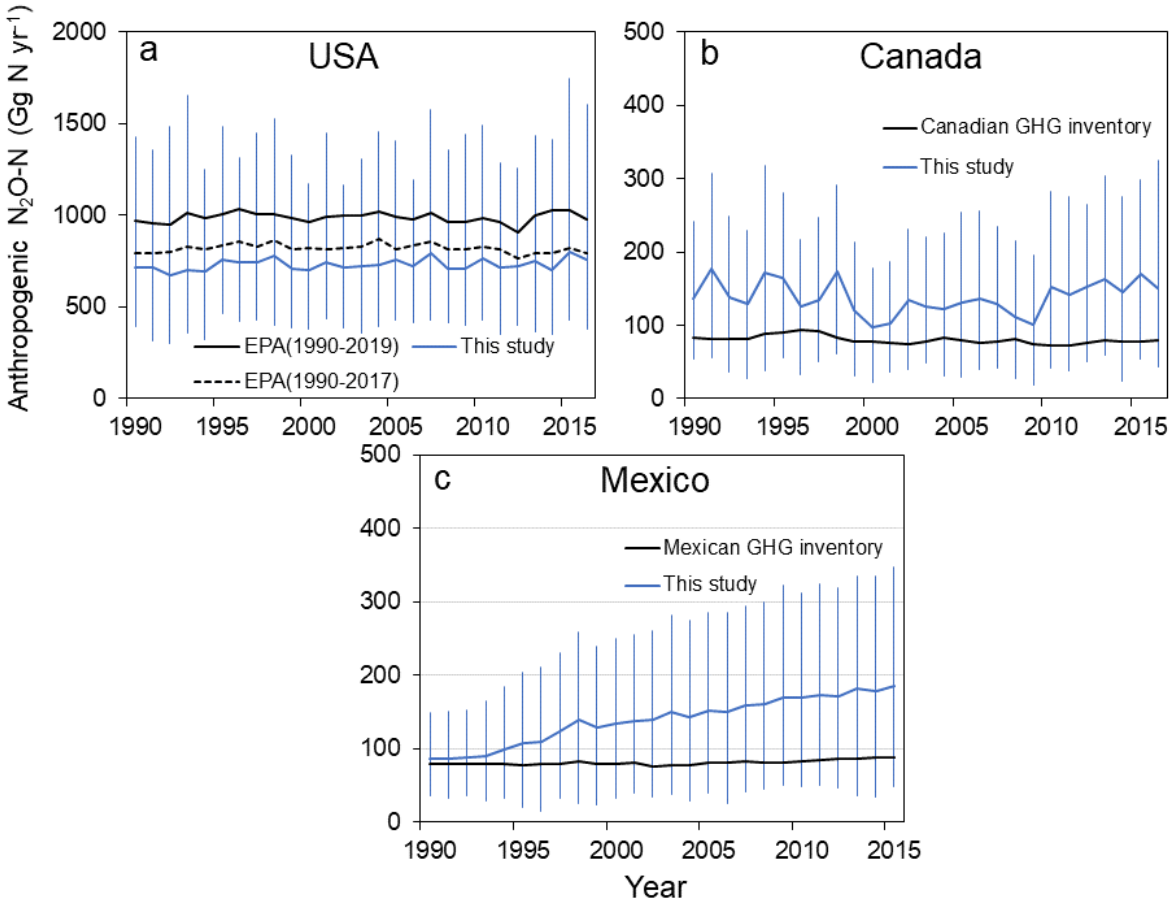

Figure 4. Comparison of our anthropogenic N_2O emissions from BU estimates with national GHG inventories during 1990–2016: **a,** EPA; **b,** Canadian GHG inventory; **c,** Mexican GHG inventory.

In addition, we compared anthropogenic N_2O emissions from our BU approaches with national inventories for the U.S., Canada, and Mexico during 1990–2016. There remain large uncertainties in estimates from different BU approaches. Our total anthropogenic N_2O emission is on average 90 Gg N yr^{-1} lower than that from the U.S. Environmental Protection Agency (EPA, Figure 4a) 1990–2017 inventory reported in 2019, which is attributed to two times lower inventory-based agricultural emissions from FAOSTAT, EDGARv4.3.2 and GAINS compared

to EPA and NMIP results (Figure S2a). The EPA 1990–2017 inventory of agricultural N_2O emissions, which adopted a Tier3 approach based on the DayCent model for emissions from agricultural soils, is more consistent with our tier3, model-based (NMIP) estimates and trends. Recently, U.S. EPA extended anthropogenic N_2O emissions to 2019. The estimate of anthropogenic N_2O emissions in the 1990–2019 inventory increased by 20% compared to the 1990–2017 inventory, which is due to a 21% higher estimate of agricultural soil emissions from the model improvement of freeze-thaw cycles in DayCent (Del Grosso, 2010, 2018) and a 330% higher estimate of waste emissions based on the revised domestic wastewater N_2O methodology according to the IPCC 2019 Refinement (IPCC, 2019) (Figures 4a, S2a,d). When comparing agricultural N_2O emissions, our NMIP results are on average 130 Gg N yr^{-1} lower than the EPA 1990–2019 inventory, consistent with the fact that some of NMIP models might underestimate agricultural soil N_2O emissions due to missing freeze-thaw cycles. Our estimates of N_2O emissions from fossil fuel and industry roughly agree with EPA-reported magnitudes and trends during 1990–2016 (Figures S2b, c).

By contrast, our total anthropogenic N_2O emissions in Canada and Mexico, which reveal significant inter-annual variability, are on average 60 Gg N yr^{-1} higher than estimates from the Canadian GHG inventory between 1990 and 2016 (Figure 4b) and the Mexican GHG inventory between 1990 and 2015 (Figure 4c), respectively. In both countries, NMIP agricultural emissions were twice as high as the four inventories (Figures S3a & S4a). Our estimates of N_2O emissions from fossil fuel and industry showed a decrease during 1990–2016, and roughly agreed with the Canadian GHG inventory in terms of both magnitudes and trends (Figures S3b, c). Mexican industrial emissions of N_2O (primarily from chemical production) increased by a factor of ~60 since 1990, based on the estimate from EDGARv4.3.2 (Janssens-Maenhout et al. 2019), however, this massive increase was not observed in GAINS and the Mexican GHG inventory. Specifically, we found a threefold increase in industrial N_2O emissions reported by GAINS (Winiwarter, 2005; Winiwarter et al., 2018), but a fourfold decrease by the Mexican GHG inventory during 1990–2010, and both inventories were almost equal thereafter until 2015 (Figure S4b). The considerably large but uncertain contribution from Mexican industrial emissions over the recent decades reported by EDGARv4.3.2 needs more investigation.

Agriculture is the largest anthropogenic N_2O emission source in the U.S. and Canada, owing to N inputs to cropland and pasture. Model-based direct soil N_2O emissions showed a faster increasing trend with two times larger values compared with inventory-based estimates that were calculated based on the use of constant EFs (Figure S8). Along with rising N additions to agricultural soils (T. J. Griffis et al., 2017; Pärn et al., 2018; Smith, 1997; Tian et al., 2019), global warming may have elevated soil nitrification and denitrification processes, especially in boreal regions (e.g., Canada), thus also contributing to faster growth in N_2O emissions. On the other hand, the assumed linear response of agricultural soil emissions to N fertilizer use may not realistically represent real-world emissions under varied climate and soil conditions (Shcherbak et al., 2014; Wang et al., 2019). The interactive effect between climate change and N additions as well as spatiotemporal variability in environmental factors such as rainfall and temperature can modulate the N_2O yield from nitrification and denitrification. Moreover, EF-based inventories that fail to consider the legacy effect due to the long-term human-added N accumulation in soils may lead to an underestimate of agricultural soil N_2O emissions (Thompson et al., 2019).

3.4 Implications for Future Research

Large uncertainties that remain in both TD and BU approaches need further investigation. Inversion models are based on atmospheric N_2O data measured by global and regional monitoring networks and aircraft campaigns. Atmospheric inversions rely on a priori estimates that may include inventory-based and model-based N_2O emissions from natural and agricultural soils, oceans, industry, and biomass burning (Nevison et al., 2018; Thompson et al., 2014). For instance, we included two estimates from PYVAR-CAMS since two different ocean prior fluxes were used. A high ocean prior flux used in PYVAR-CAMS-1 led to a low land flux. In addition, more available measurement sites and expanded network coverage would improve inversion accuracy. The estimates of the CT-L regional inversion were improved partially because it uses a substantially larger set of North American measurements, particularly NOAA aircraft data over the Midwest, and uses a higher resolution of the transport models compared with global inversion models. Furthermore, more spatially accurate prior flux estimates will improve confidence in the inversion results. BU estimates in our synthesis were not employed as prior fluxes for the four inversion models. Moreover, the prior fluxes used in the four TD models were from different data sources (Thompson et al., 2019). Future work should use the currently synthesized BU estimates as a priori estimates in the TD framework to reconcile the inversions with BU calculations. There remains large uncertainty in agricultural soil N_2O emissions from the process-based ecosystem models (Tian et al., 2019). First, this large uncertainty among models is associated with different representations of biogeochemical processes and the omission or simplification of agricultural practices. For instance, most NMIP models have not considered the freeze-thaw cycle in soils. It has been reported that freeze-thaw cycles could contribute to 17%~28% more of global agricultural N_2O emissions (Wagner-Riddle et al., 2017). The new freeze-thaw version of DayCent model showed a 21% more N_2O emission from U.S. agriculture during 1990–2019 compared to its previous simulations, which was higher than NMIP results. Second, model uncertainties in predicting cropland N_2O emissions would be reduced through improved representation of geospatial data and sub-national statistics to describe agricultural practices more precisely like legume cultivation, rotation, tillage, and cover-crops. Third, NMIP models' responses to different driving factors are divergent. Future research to improve accuracy in model-based N_2O emissions should include single-factor model validations against field experiments.

4 Conclusions

North American N_2O emissions estimated by BU approaches (1.7 Tg N yr^{-1} during 2007–2016) were on average 0.4 Tg N yr^{-1} larger than the corresponding TD estimates in this study; however, our mean BU estimate was roughly consistent with the CT-L regional inversion model in Nevison et al. (2018). Anthropogenic emissions were the major contributor to the total North American N_2O source, and were dominated (68%) by agriculture and industry. Agriculture is the largest overall N_2O source and is attributable to soil N additions. The recent estimates from NMIP and DayCent models showed that N_2O directly emitted from agricultural soils has exhibited a faster increase in recent years than predicted by EF-based national GHG inventories. We speculate that EF-based inventories may underestimate agricultural N_2O emissions due to omission of interactive effects of environmental change and N additions, and legacy impacts of long-term soil N accumulations. There remains uncertainty in TD and BU estimates of N_2O at both annual and seasonal time scales. For example, Nevison et al. (2018) emphasized that the

Midwestern Corn/Soybean Belt was a hotspot of N_2O emission in North America, although this was not found with our global atmospheric inversions, albeit they all estimated above average emissions in the region. It is likely due to the smaller number of observations over the Midwest used in the global estimates, the longer time frame of global inversions that diluted the impact of Midwestern sites, and much coarser resolutions of transport models used in global inversions. On the other hand, high N_2O emissions were simulated to different degrees in the Midwestern U.S. by the six BU terrestrial biosphere models used here.

We reported North American N_2O emissions based on both TD and BU approaches and provided new insights into strengths and limitations of each approach for reducing future uncertainty. To reconcile the large divergence between TD and BU estimates, we recommend that more consistent and accurate prior fluxes, more available measurement sites, and expanded network coverage should be considered to improve the accuracy of atmospheric inversions. Meanwhile, improved representation and validation of biogeochemical processes (e.g., freeze-thaw and dry-wet cycles) and better geospatial data and statistics on agricultural practices (e.g., legume cultivation, rotation, tillage, and cover-cropped system) could pave the way for better simulation of daily and cumulative soil N_2O emissions.

Acknowledgments

This research has been supported partly by NSF grant nos. 1903722, 1922687; NOAA grant nos. NA16NOS4780207 and NA16NOS4780204, Andrew Carnegie Fellowship Award no. G-F-19-56910. Additional funding support includes: R.L.T. and P.R. acknowledge funding support from VERIFY project (EC H2020 grant no. 776810). P.C. acknowledges support from ERC SyG GrantImbalance-P. P.C. and R.L, acknowledge support from the ANR Cland convergence institute. A.I. acknowledges funding support from JSPS KAKENHI grant (no. 17H01867). F.J. and S.L. acknowledge support by Swiss National Science Foundation (# #200020_200511) and by the EC H2020 grant no. 821003 (Project 4C) and no. 820989 (Project COMFORT). The work reflects only the authors' view; the European Commission and their executive agency are not responsible for any use that may be made of the information the work contains. P.K.P. is partly supported by Environment Research and Technology Development Fund (#2-1802) of the Ministry of the Environment, Japan. K.C.W. and D.B.M. acknowledge support from NASA (IDS Grant #NNX17AK18G) and NOAA (Grant #NA13OAR4310086). P.A.R. acknowledges NASA Award NNX17AI74G. F.N.T. acknowledges funding from FAO regular programme. The views expressed in this publication are those of the author(s) and do not necessarily reflect the views or policies of FAO. S.Z. acknowledges support by the EC H2020 grant no. 647204. F.Z. acknowledges the support from the National Natural Science Foundation of China (41671464). We acknowledge Greet Janssens-Maenhout for providing EDGAR N_2O emission data and Alexander F Bouwman for providing aquacultural N_2O emission data. This work contributes to the REgional Carbon Cycle Assessment and Porcesses-2 of the Global Carbon Project. The relevant datasets of this study are archived in the box site at Auburn University (https://auburn.box.com/s/csi2vkgrgcd267rxlvm97jnncrcx0hqi).

References

Beusen, A. H., Bouwman, A. F., Van Beek, L. P., Mogollón, J. M., & Middelburg, J. J. (2016). Global riverine N and P transport to ocean increased during the 20th century despite increased retention along the aquatic continuum. *Biogeosciences, 13*(8), 2441-2451.

Bouwman, A. F., Beusen, A., Overbeek, C., Bureau, D., Pawlowski, M., & Glibert, P. (2013). Hindcasts and future projections of global inland and coastal nitrogen and phosphorus loads due to finfish aquaculture. *Reviews in Fisheries Science, 21*(2), 112-156.

Chen, Z., Griffis, T. J., Millet, D. B., Wood, J. D., Lee, X., Baker, J. M., et al. (2016). Partitioning N_2O emissions within the US Corn Belt using an inverse modeling approach. *Global Biogeochemical Cycles, 30*(8), 1192-1205.

Ciais, P., Sabine, C., Bala, G., Bopp, L., Brovkin, V., Canadell, J., et al. (2014). Carbon and other biogeochemical cycles. In *Climate Change 2013: The Physical Science Basis. Contribution of Working Group I to the Fifth Assessment Report of the Intergovernmental Panel on Climate Change* (pp. 465-570): Cambridge University Press.

Dangal, S. R., Tian, H., Xu, R., Chang, J., Canadell, J. G., Ciais, P., et al. (2019). Global nitrous oxide emissions from pasturelands and rangelands: Magnitude, spatio-temporal patterns and attribution. *Global Biogeochemical Cycles, 33*, 200-222.

Del Grosso, S., Ogle, S., Parton, W., & Breidt, F. (2010). Estimating uncertainty in N_2O emissions from US cropland soils. *Global Biogeochemical Cycles, 24*(1).

Del Grosso, S. J. (2010). Grazing and nitrous oxide. *Nature, 464*(7290), 843-844. https://doi.org/10.1038/464843a

Del Grosso, S. J., Ogle, S. M., Parton, W. J., Nevison, C. D., Smith, W., Grant, B., et al. (2018). *Comparing soil nitrous oxide emissions simulated by the new freeze-thaw version of daycent with fluxes inferred from atmospheric inversion.* Paper presented at the AGU Fall Meeting Abstracts.

Du, E., de Vries, W., Han, W., Liu, X., Yan, Z., & Jiang, Y. (2016). Imbalanced phosphorus and nitrogen deposition in China's forests. *Atmospheric Chemistry and Physics, 16*(13), 8571.

Eyring, V., Lamarque, J.-F., Hess, P., Arfeuille, F., Bowman, K., Chipperfiel, M. P., et al. (2013). Overview of IGAC/SPARC Chemistry-Climate Model Initiative (CCMI) community simulations in support of upcoming ozone and climate assessments. *40*(Januar), 48-66.

FAO. (2021). FAOSTAT, database of the Food and Agriculture Organization of the United Nations Statistics. Data avaialble as follows:Livestock Manure: http://www.fao.org/faostat/en/#data/EMN ; Emissions totals: http://www.fao.org/faostat/en/#data/GT; population: http://www.fao.org/faostat/en/#data/OA

FAO(2020). Livestock and environment statistics: manure and greenhouse gas emissions. Global, regional and country trends, 1990–2018. FAOSTAT Analytical Brief Series No. 14. Rome. http://www.fao.org/3/cb1922en/cb1922en.pdf

Griffis, T., Lee, X., Baker, J., Russelle, M., Zhang, X., Venterea, R., & Millet, D. (2013). Reconciling the differences between top-down and bottom-up estimates of nitrous oxide emissions for the US Corn Belt. *Global Biogeochemical Cycles, 27*(3), 746-754. https://doi.org/10.1002/gbc.20066

Griffis, T. J., Chen, Z., Baker, J. M., Wood, J. D., Millet, D. B., Lee, X., et al. (2017). Nitrous oxide emissions are enhanced in a warmer and wetter world. *Proceedings of the National Academy of Sciences, 114*(45), 12081-12085. https://doi.org/10.1073/pnas.1704552114

Hurtt, G., Chini, L. P., Frolking, S., Betts, R., Feddema, J., Fischer, G., et al. (2011). Harmonization of land-use scenarios for the period 1500–2100: 600 years of global gridded annual land-use transitions, wood harvest, and resulting secondary lands. *Climatic Change, 109*(1-2), 117-161. DOI 10.1007/s10584-011-0153-2

IPCC. (2006). *2006 IPCC Guidelines for National Greenhouse Gas Inventories.* Retrieved from Hayama, Japan.

IPCC. (2019). *2019 Refinement to the 2006 IPCC Guidelines for National Greenhouse Gas Inventories.*Vol. 4 (IPCC, 2019).

Janssens-Maenhout, G., Crippa, M., Guizzardi, D., Muntean, M., Schaaf, E., Dentener, F., et al. (2019). EDGAR v4.3.2 Global Atlas of the three major greenhouse gas emissions for the period 1970–2012. *Earth System Science Data, 11*(3), 959-1002. https://www.earth-syst-sci-data.net/11/959/2019/

Kort, E. A., Eluszkiewicz, J., Stephens, B. B., Miller, J. B., Gerbig, C., Nehrkorn, T., et al. (2008). Emissions of CH_4 and N_2O over the United States and Canada based on a receptor-oriented modeling framework and COBRA-NA atmospheric observations. *Geophysical Research Letters, 35*(18). https://doi.org/10.1029/2008GL034031

Lauerwald, R., Regnier, P., Figueiredo, V., Enrich-Prast, A., Bastviken, D., Lehner, B., et al. (2019). Natural lakes are a minor global source of N_2O to the atmosphere. *Global Biogeochemical Cycles, 33*, 1564-1581. https://doi.org/10.1111/gcb.14928

Lu, C., & Tian, H. (2017). Global nitrogen and phosphorus fertilizer use for agriculture production in the past half century: shifted hot spots and nutrient imbalance. *Earth System Science Data, 9*(1), 181-192. https://doi.org/10.5194/essd-9-181-2017

Maavara, T., Lauerwald, R., Laruelle, G. G., Akbarzadeh, Z., Bouskill, N. J., Van Cappellen, P., & Regnier, P. (2019). Nitrous oxide emissions from inland waters: Are IPCC estimates too high? *Global Change Biology, 25*(2), 473-488.

MacLeod, M., Hasan, M. R., Robb, D. H. F., & Mamun-Ur-Rashid, M. (2019). *Quantifying and mitigating greenhouse gas emissions from global aquaculture*. Retrieved from Rome.

McDaniel, M. D., Saha, D., Dumont, M., Hernández, M., & Adams, M. (2019). The effect of land-use change on soil CH 4 and N 2 O fluxes: a global meta-analysis. *Ecosystems, 22*(6), 1424-1443.

Meurer, K. H., Franko, U., Stange, C. F., Dalla Rosa, J., Madari, B. E., & Jungkunst, H. F. (2016). Direct nitrous oxide (N2O) fluxes from soils under different land use in Brazil—a critical review. *Environmental Research Letters, 11*(2), 023001.

Miller, S., Kort, E., Hirsch, A., Dlugokencky, E., Andrews, A., Xu, X., et al. (2012). Regional sources of nitrous oxide over the United States: Seasonal variation and spatial distribution. *Journal of Geophysical Research: Atmospheres, 117*(D6).

Nevison, C., Andrews, A., Thoning, K., Dlugokencky, E., Sweeney, C., Miller, S., et al. (2018). Nitrous Oxide Emissions Estimated With the CarbonTracker-Lagrange North American Regional Inversion Framework. *Global Biogeochemical Cycles, 32*(3), 463-485.

Pärn, J., Verhoeven, J. T., Butterbach-Bahl, K., Dise, N. B., Ullah, S., Aasa, A., et al. (2018). Nitrogen-rich organic soils under warm well-drained conditions are global nitrous oxide emission hotspots. *Nature Communications, 9*(1), 1135.

Patra, P. K., Takigawa, M., Watanabe, S., Chandra, N., Ishijima, K., & Yamashita, Y. (2018). Improved chemical tracer simulation by MIROC4. 0-based atmospheric chemistry-transport model (MIROC4-ACTM). *Sola, 14*, 91-96.

Prinn, R. G., Weiss, R. F., Arduini, J., Arnold, T., DeWitt, H. L., Fraser, P. J., et al. (2018). History of chemically and radiatively important atmospheric gases from the Advanced Global Atmospheric Gases Experiment (AGAGE). *Earth System Science Data, 10*(2), 985-1018. https://www.earth-syst-sci-data.net/10/985/2018/

Saikawa, E., Prinn, R., Dlugokencky, E., Ishijima, K., Dutton, G., Hall, B., et al. (2014). Global and regional emissions estimates for N_2O. *Atmospheric Chemistry and Physics, 14*, 4617-4641, https://doi.org/10.5194/acp-14-4617-2014.

Shang, Z., Zhou, F., Smith, P., Saikawa, E., Ciais, P., Chang, J., et al. (2019). Weakened growth of cropland-N_2O emissions in China associated with nationwide policy interventions. *Global Change Biology, 25*(11), 3706-3719. https://onlinelibrary.wiley.com/doi/abs/10.1111/gcb.14741

Shcherbak, I., Millar, N., & Robertson, G. P. (2014). Global metaanalysis of the nonlinear response of soil nitrous oxide (N_2O) emissions to fertilizer nitrogen. *Proceedings of the National Academy of Sciences, 111*(25), 9199-9204.

Smith, K. (1997). The potential for feedback effects induced by global warming on emissions of nitrous oxide by soils. *Global change biology, 3*(4), 327-338.

Stehfest, E., & Bouwman, L. (2006). N_2O and NO emission from agricultural fields and soils under natural vegetation: summarizing available measurement data and modeling of global annual emissions. *Nutrient Cycling in Agroecosystems, 74*(3), 207-228.

Thompson, R. L., Chevallier, F., Crotwell, A. M., Dutton, G. S., Langenfelds, R. L., Prinn, R. G., et al. (2014). Nitrous oxide emissions 1999 to 2009 from a global atmospheric inversion. *Atmospheric Chemistry and Physics, 14*, 1801-1817, https://doi.org/10.5194/acp-14-1801-2014.

Thompson, R. L., Lassaletta, L., Patra, P. K., Wilson, C., Wells, K. C., Gressent, A., et al. (2019). Acceleration of global N_2O emissions seen from two decades of atmospheric inversion. *Natural Climate Change, 9*, 993-998.

Tian, H., Lu, C., Ciais, P., Michalak, A. M., Canadell, J. G., Saikawa, E., et al. (2016). The terrestrial biosphere as a net source of greenhouse gases to the atmosphere. *Nature, 531*(7593), 225-228. https://doi.org/10.1038/nature16946

Tian, H., Xu, R., Canadell, J. G., Thompson, R. L., Winiwarter, W., Suntharalingam, P., et al. (2020a). A comprehensive quantification of global nitrous oxide sources and sinks. *Nature*, *586*(7828), 248-256. https://doi.org/10.1038/s41586-020-2780-0

Tian, H., Xu, R., Pan, S., Yao, Y., Bian, Z., Cai, W.-J., et al. (2020b). Long-Term Trajectory of Nitrogen Loading and Delivery From Mississippi River Basin to the Gulf of Mexico. *Global Biogeochemical Cycles*, *34*(5), e2019GB006475. https://doi.org/10.1029/2019GB006475

Tian, H. Q., Yang, J., Xu, R. T., Lu, C. Q., Canadell, J. G., Davidson, E. A., et al. (2019). Global soil nitrous oxide emissions since the preindustrial era estimated by an ensemble of terrestrial biosphere models: Magnitude, attribution, and uncertainty. *Global Change Biology*, *25*(2), 640-659.

Tubiello, F., Cóndor-Golec, R., Salvatore, M., Piersante, A., Federici, S., Ferrara, A., et al. (2015). *Estimating greenhouse gas emissions in agriculture: a manual to address data requirements for developing countries*. http://www.fao.org/3/i4260e/i4260e.pdf

Tubiello, F.N., 2019. GHG Emissions due to agriculture. Encyclopedia of Food Security and Sustainability, Volume 1, 2019, Pages 196-205, https://doi.org/10.1016/B978-0-08-100596-5.21996-3

Van Der Werf, G. R., Randerson, J. T., Giglio, L., Van Leeuwen, T. T., Chen, Y., Rogers, B. M., et al. (2017). Global fire emissions estimates during 1997-2016. *Earth System Science Data*, *9*, 697-720.

van Lent, J., Hergoualc'h, K., & Verchot, L. V. (2015). Reviews and syntheses: Soil N 2 O and NO emissions from land use and land-use change in the tropics and subtropics: a meta-analysis. *Biogeosciences*, *12*(23), 7299-7313.

Verchot, L. V., Davidson, E. A., Cattânio, H., Ackerman, I. L., Erickson, H. E., & Keller, M. (1999). Land use change and biogeochemical controls of nitrogen oxide emissions from soils in eastern Amazonia. *Global Biogeochemical Cycles*, *13*(1), 31-46. https://agupubs.onlinelibrary.wiley.com/doi/abs/10.1029/1998GB900019

Wagner-Riddle, C., Congreves, K. A., Abalos, D., Berg, A. A., Brown, S. E., Ambadan, J. T., et al. (2017). Globally important nitrous oxide emissions from croplands induced by freeze–thaw cycles. *Nature Geoscience*, *10*(4), 279-283. https://doi.org/10.1038/ngeo2907

Wang, Q., Zhou, F., Shang, Z., Ciais, P., Winiwarter, W., Jackson, R. B., et al. (2019). Data-driven estimates of global nitrous oxide emissions from croplands. *National Science Review*, *00*, 1-12.

Wells, K. C., Millet, D. B., Bousserez, N., Henze, D. K., Chaliyakunnel, S., Griffis, T. J., et al. (2015). Simulation of atmospheric N₂O with GEOS-Chem and its adjoint: evaluation of observational constraints. *Geosci. Model Dev.*, *8*(10), 3179-3198. https://www.geosci-model-dev.net/8/3179/2015/

Williams, J., & Crutzen, P. J. (2010). Nitrous oxide from aquaculture. *Nature Geoscience*, *3*, 143. Correspondence. https://doi.org/10.1038/ngeo804

Wilson, C., Chipperfield, M., Gloor, M., & Chevallier, F. (2014). Development of a variational flux inversion system (INVICAT v1. 0) using the TOMCAT chemical transport model. *Geoscientific Model Development*, *7*, 2485-2500.

Winiwarter, W. (2005). The GAINS model for greenhouse gases-version 1.0: nitrous oxide (N_2O).

Winiwarter, W., Höglund-Isaksson, L., Klimont, Z., Schöpp, W., & Amann, M. (2018). Technical opportunities to reduce global anthropogenic emissions of nitrous oxide. *Environmental Research Letters*, *13*(1), 014011.

Xu, R., Tian, H., Pan, S., Dangal, S. R., Chen, J., Chang, J., et al. (2019). Increased nitrogen enrichment and shifted patterns in the world's grassland: 1860–2016. *Earth System Science Data*, *11*(1), 175-187.

Xu, X., Tian, H., Chen, G., Liu, M., Ren, W., Lu, C., & Zhang, C. (2012). Multifactor controls on terrestrial N_2O flux over North America from 1979 through 2010. *Biogeosciences*, *9*(4), 1351-1366.

Yao, Y., Tian, H., Shi, H., Pan, S., Xu, R., Pan, N., & Canadell, J. G. (2020). Increased global nitrous oxide emissions from streams and rivers in the Anthropocene. *Natural Climate Change*, *10*(2), 138-142.

Zaehle, S., Ciais, P., Friend, A. D., & Prieur, V. (2011). Carbon benefits of anthropogenic reactive nitrogen offset by nitrous oxide emissions. *Nature Geoscience*, *4*, 601-605.

Zhang, B., Tian, H., Lu, C., Dangal, S. R., Yang, J., & Pan, S. (2017). Global manure nitrogen production and application in cropland during 1860–2014: a 5 arcmin gridded global dataset for Earth system modeling. *Earth System Science Data*, *9*(2).

Geophysical Research Letters

Supporting Information for

Magnitude and uncertainty in nitrous oxide emissions from North America based on bottom-up and top-down approaches

R. Xu[1,2], H. Tian[1], N. Pan[1], R. L. Thompson[3], J. G. Canadell[4], E. A. Davidson[5], C. Nevison[6], W. Winiwarter[7,8], H. Shi[1], S. Pan[1], J. Chang[9], P. Ciais[10], S. R. S. Dangal[11], A. Ito[12], R. B. Jackson[13], F. Joos[14], R. Lauerwald[15], S. Lienert[14], T. Maavara[16], D. B. Millet[17], P. A. Raymond[16], P. Regnier[18], F. N. Tubiello[19], N. Vuichard[10], K. C. Wells[17], C. Wilson[20,21], J. Yang[22], Y. Yao[1], S. Zaehle[23], F. Zhou[24]

[1]International Center for Climate and Global Change Research, School of Forestry and Wildlife Sciences, Auburn University, Auburn, AL, USA.
[2]Forest Ecosystems and Society, Oregon State University, Corvallis, OR, USA.
[3]Norsk Institutt for Luftforskning, NILU, Kjeller, Norway.
[4]Global Carbon Project, CSIRO Oceans and Atmosphere, Canberra, Australia.
[5]Appalachian Laboratory, University of Maryland Center for Environmental Science, Frostburg, MD, USA.
[6]University of Colorado Boulder/INSTAAR, Boulder, CO, USA.
[7]International Institute for Applied Systems Analysis, Laxenburg, Austria.
[8]Institute of Environmental Engineering, University of Zielona Góra, Zielona Góra, Poland.
[9]College of Environmental and Resource Sciences, Zhejiang University, Hangzhou, China.
[10]Laboratoire des Sciences du Climat et de l'Environnement, LSCE, CEA CNRS, UVSQ UPSACLAY, Gif sur Yvette, France.
[11]School of Natural Resources, University of Nebraska – Lincoln, NE, USA.
[12]Earth System Division, National Institute for Environmental Studies, Tsukuba, Japan.
[13]Department of Earth System Science, Woods Institute for the Environment, and Precourt Institute for Energy, Stanford University, Stanford, CA, USA.
[14]Climate and Environmental Physics, Physics Institute and Oeschger Centre for Climate Change Research, University of Bern, Bern, Switzerland.
[15]Université Paris-Saclay, INRAE, AgroParisTech, UMR ECOSYS, Thiverval-Grignon, France.
[16]Yale School of Forestry and Environmental Studies, New Haven, CT, USA.
[17]Department of Soil, Water, and Climate, University of Minnesota, MN, USA.
[18]Department Geoscience, Environment & Society-BGEOSYS, Université Libre de Bruxelles, Brussels, Belgium.
[19]Statistics Division, Food and Agriculture Organization of the United Nations, Via Terme di Caracalla, Rome, Italy.
[20]National Centre for Earth Observation, University of Leeds, Leeds, UK.
[21]Institute for Climate and Atmospheric Science, School of Earth and Environment, University of Leeds, Leeds, UK.
[22]Department of Forestry, Mississippi State University, Mississippi State, MS, USA.
[23]Max Planck Institute for Biogeochemistry, Jena, Germany.

[24]Sino-France Institute of Earth Systems Science, Laboratory for Earth Surface Processes, College of Urban and Environmental Sciences, Peking University, Beijing, China.

Corresponding author: Hanqin Tian (tianhan@auburn.edu)

Contents of this file

Figures S1 to S8
Tables S1 to S4

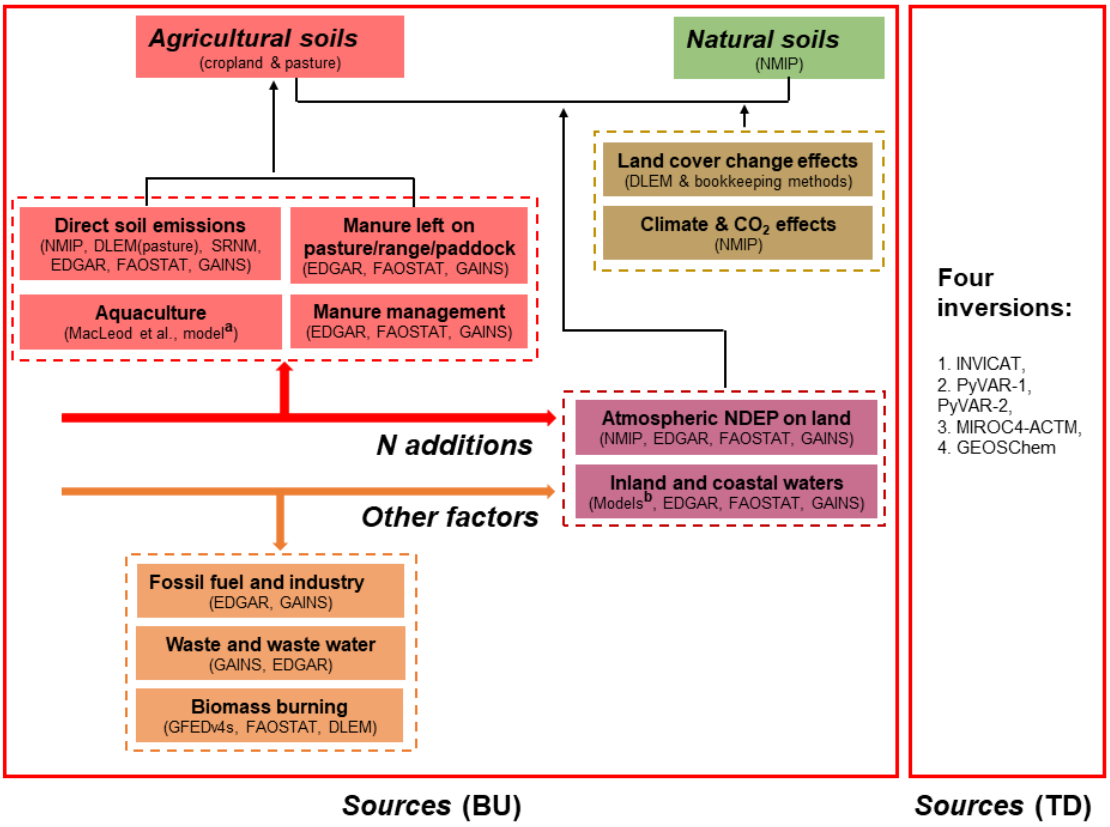

Figure S1. The methodology for data synthesis of North American N_2O sources. BU and TD represent bottom-up and top-down methods, respectively. The color codes are the same as that used in Table 1 and Figures. 1–2. We utilize both approaches, including 17 BU and five TD estimates of N_2O fluxes. For sources estimated by BU, we include six process-based terrestrial biosphere modeling studies (Tian et al., 2019); one nutrient budget model (Beusen et al., 2016; Bouwman et al., 2013; Bouwman et al., 2011); one inventory for aquaculture N_2O in 2013 (MacLeod et al., 2019); two inland water modeling studies (Lauerwald et al., 2019; Maavara et al., 2019; Yao et al., 2020); one statistical model SRNM based on spatial extrapolation of field measurements (Wang et al., 2019); and four GHG inventories: EDGAR v4.3.2 (Janssens-Maenhout et al., 2019), FAOSTAT (Tubiello et al., 2015), GAINS (Winiwarter et al., 2018), and GFED4s (Van Der Werf et al., 2017). [a]The nutrient budget model (Beusen et al., 2016; Bouwman et al., 2013; Bouwman et al., 2011) provides N flows in global freshwater and marine aquaculture over the period 1980–2016. [b]Model-based estimates of N_2O emissions from 'Inland and coastal waters' include rivers and reservoirs (Maavara et al., 2019; Yao et al., 2020), lakes (Lauerwald et al., 2019), and estuaries (Maavara et al., 2019).

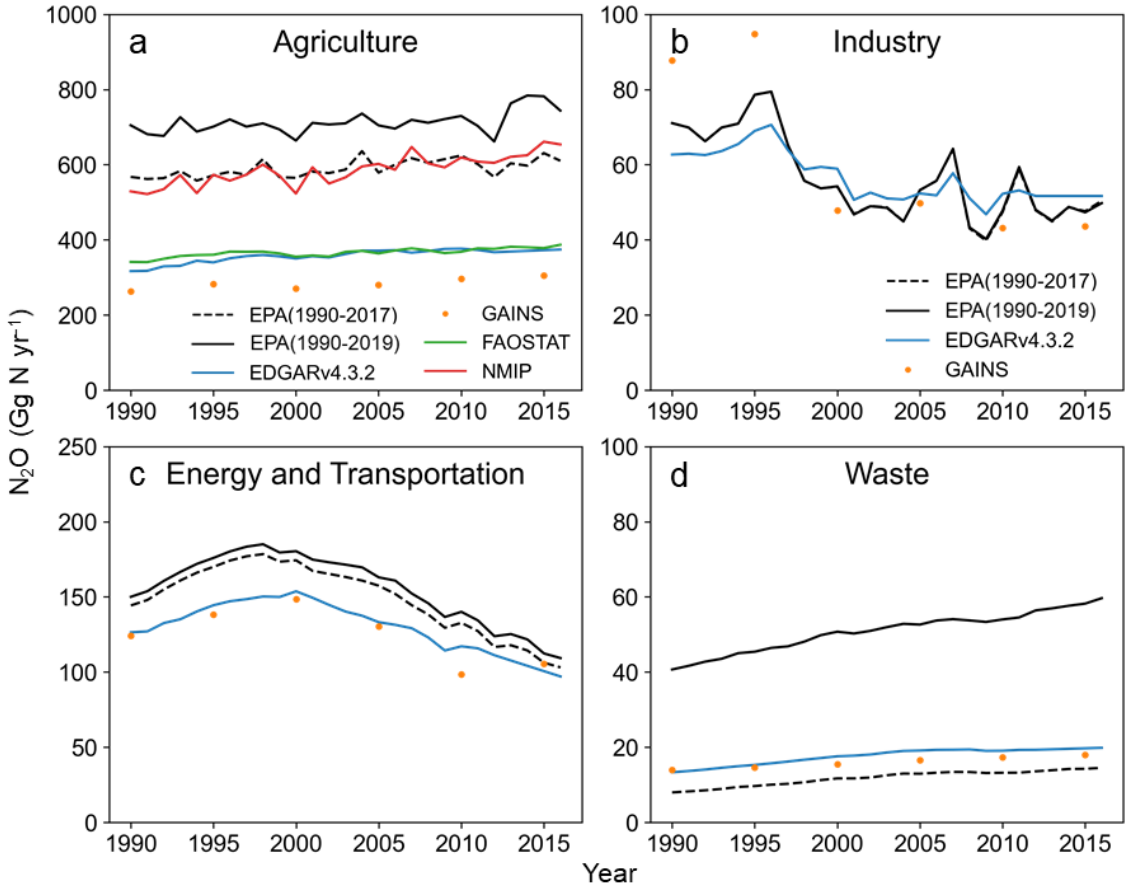

Figure S2. Comparison of our BU-estimated anthropogenic N_2O emissions with EPA during 1990–2016 in the U.S. Anthropogenic N_2O sectors include **(a)** agriculture, **(b)** industry, **(c)** energy and transportation, and **(d)** waste.

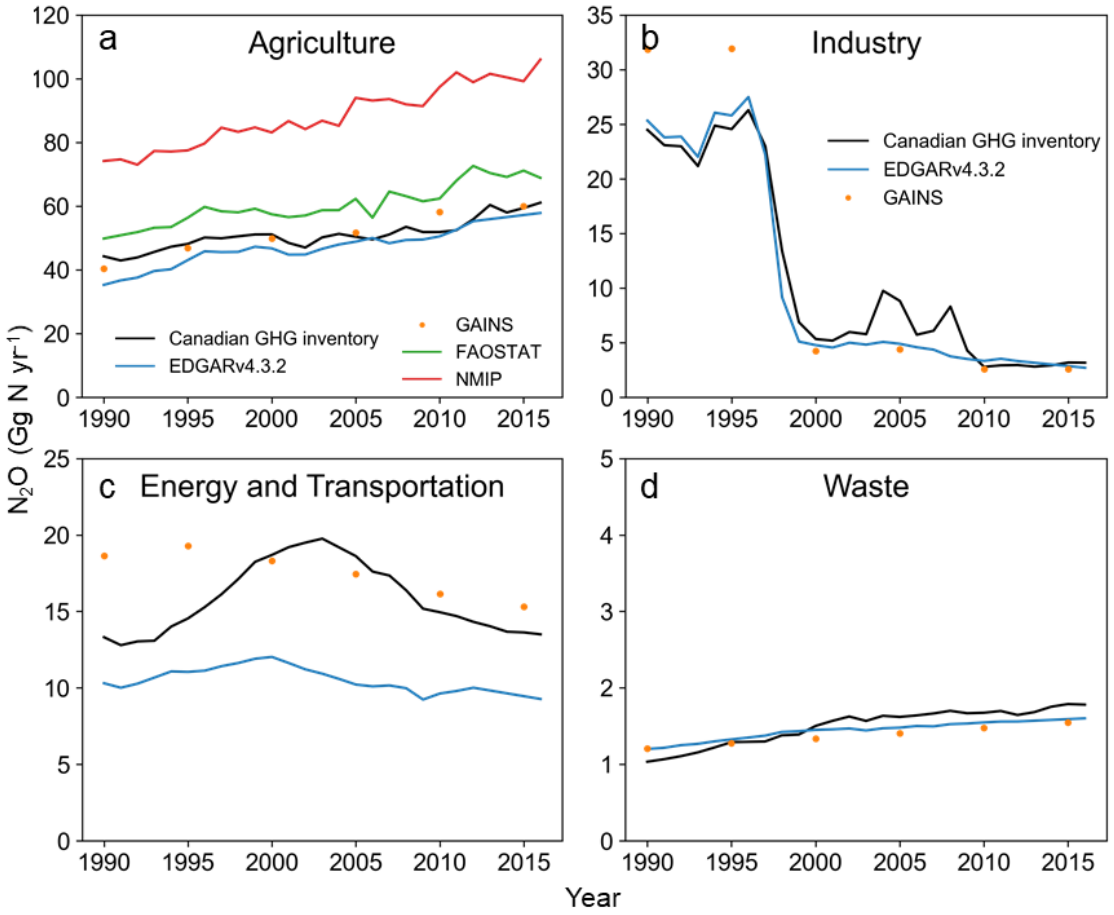

Figure S3. Comparison of our BU-estimated anthropogenic N_2O emissions with GHG inventory during 1990–2016 in Canada. Anthropogenic N_2O sectors include **(a)** agriculture, **(b)** industry, **(c)** energy and transportation, and **(d)** waste.

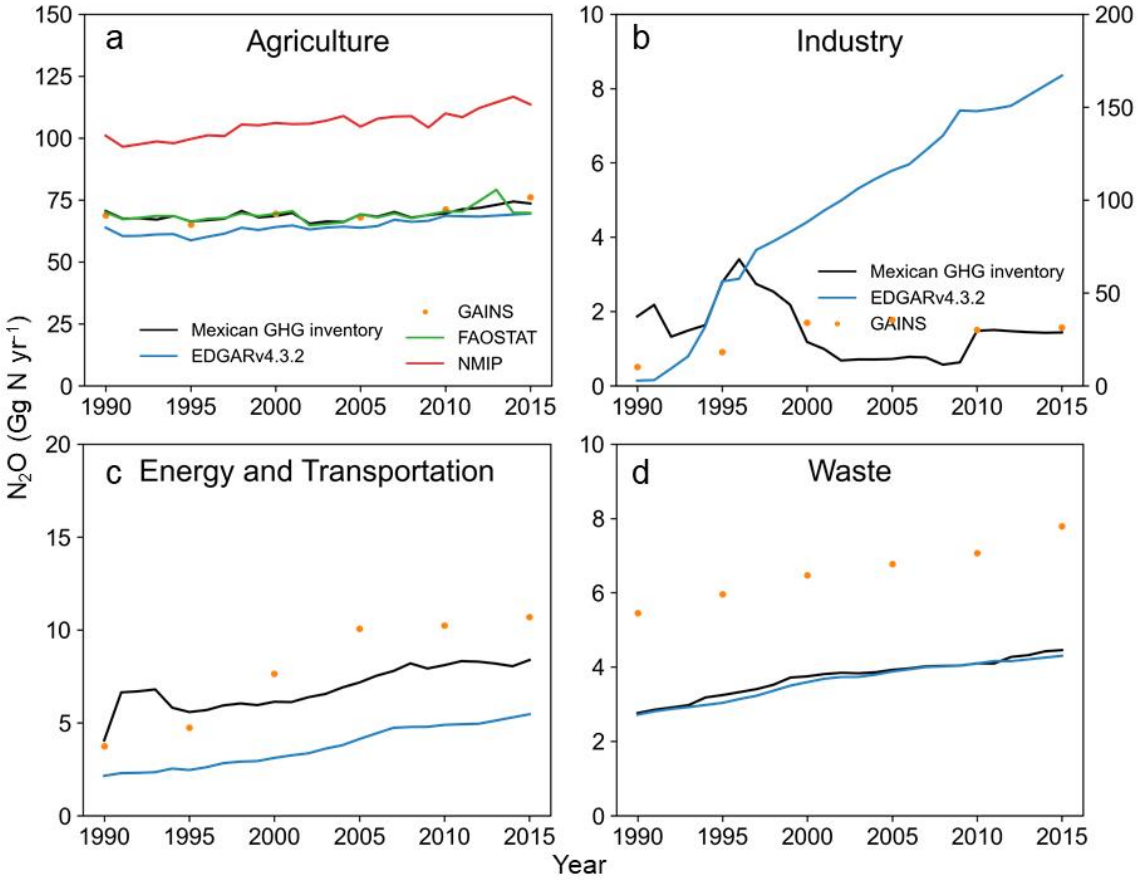

Figure S4. Comparison of our BU-estimated anthropogenic N_2O emissions with GHG inventory during 1990–2015 in Mexico. Anthropogenic N_2O sectors include **(a)** agriculture, **(b)** industry, **(c)** energy and transportation, and **(d)** waste.

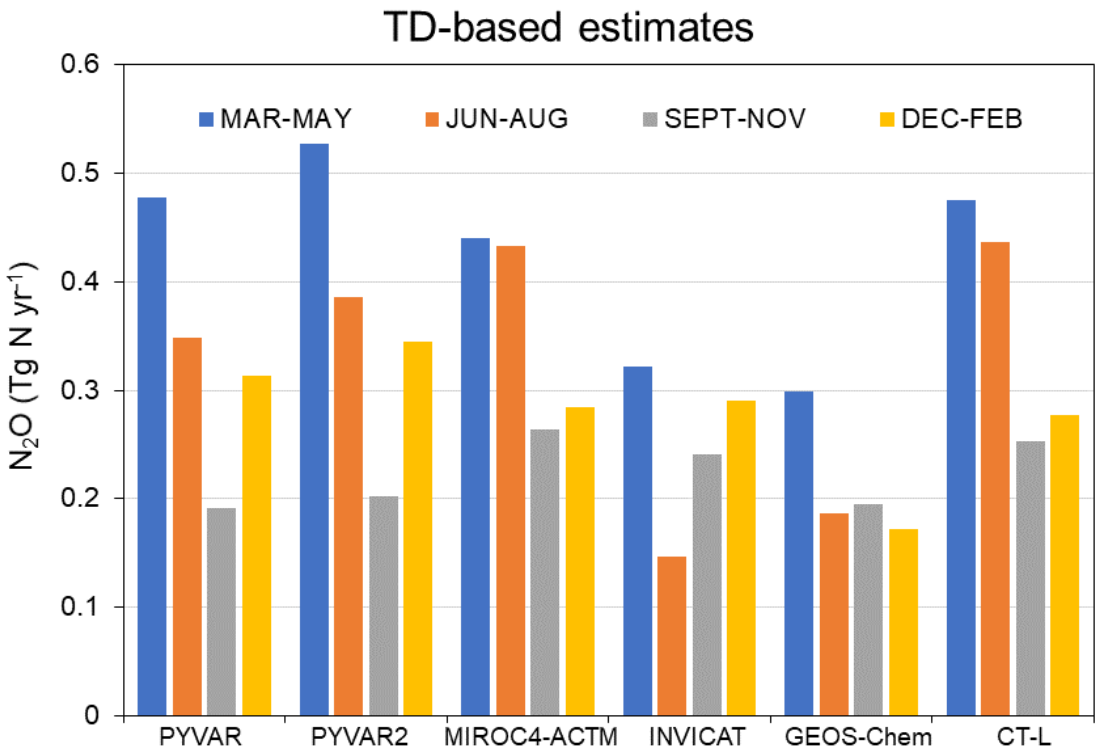

94

95 **Figure S5.** Seasonal total N_2O fluxes from TD approaches over North America between 2008
96 and 2013. Five TD inversion models include PYVAR-CAMS, MIRCO4-ACTM, INVICAT, GEOS-
97 Chem, and CT-L.

98

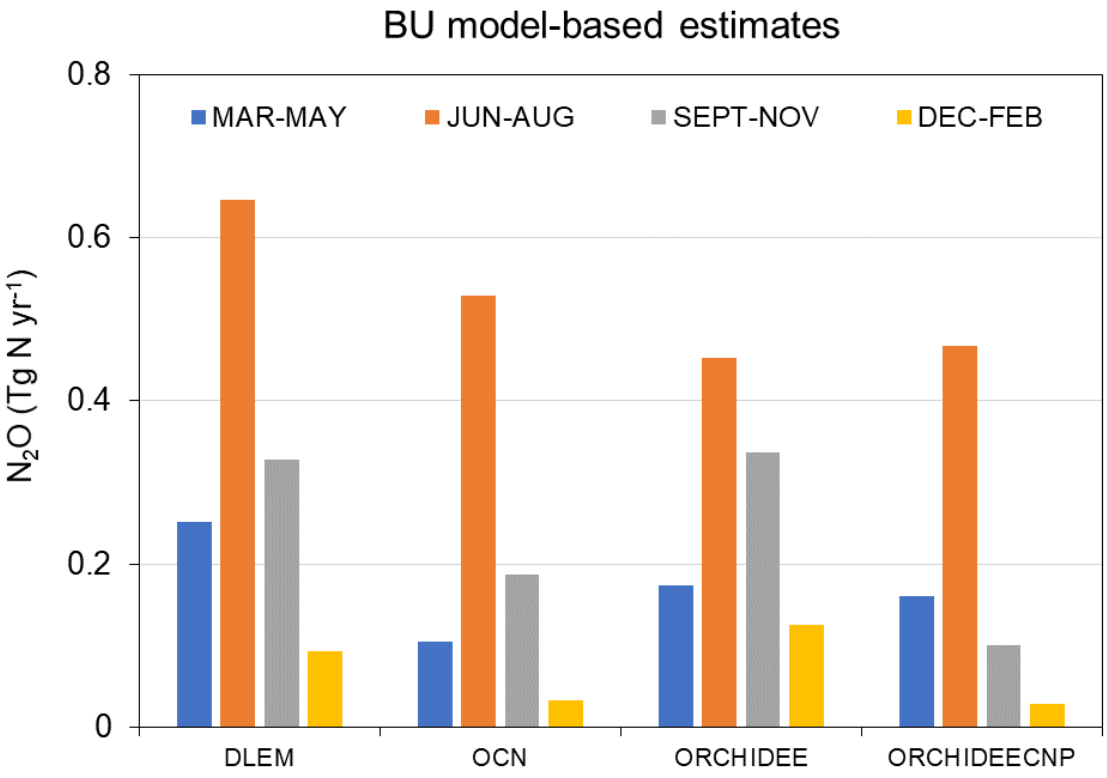

99

100 **Figure S6.** Seasonal cropland N_2O fluxes from BU approaches over North America between
101 2007 and 2016. Four terrestrial biosphere models include DLEM, OCN, ORCHIDEE, and
102 ORCHIDEE-CNP.

103

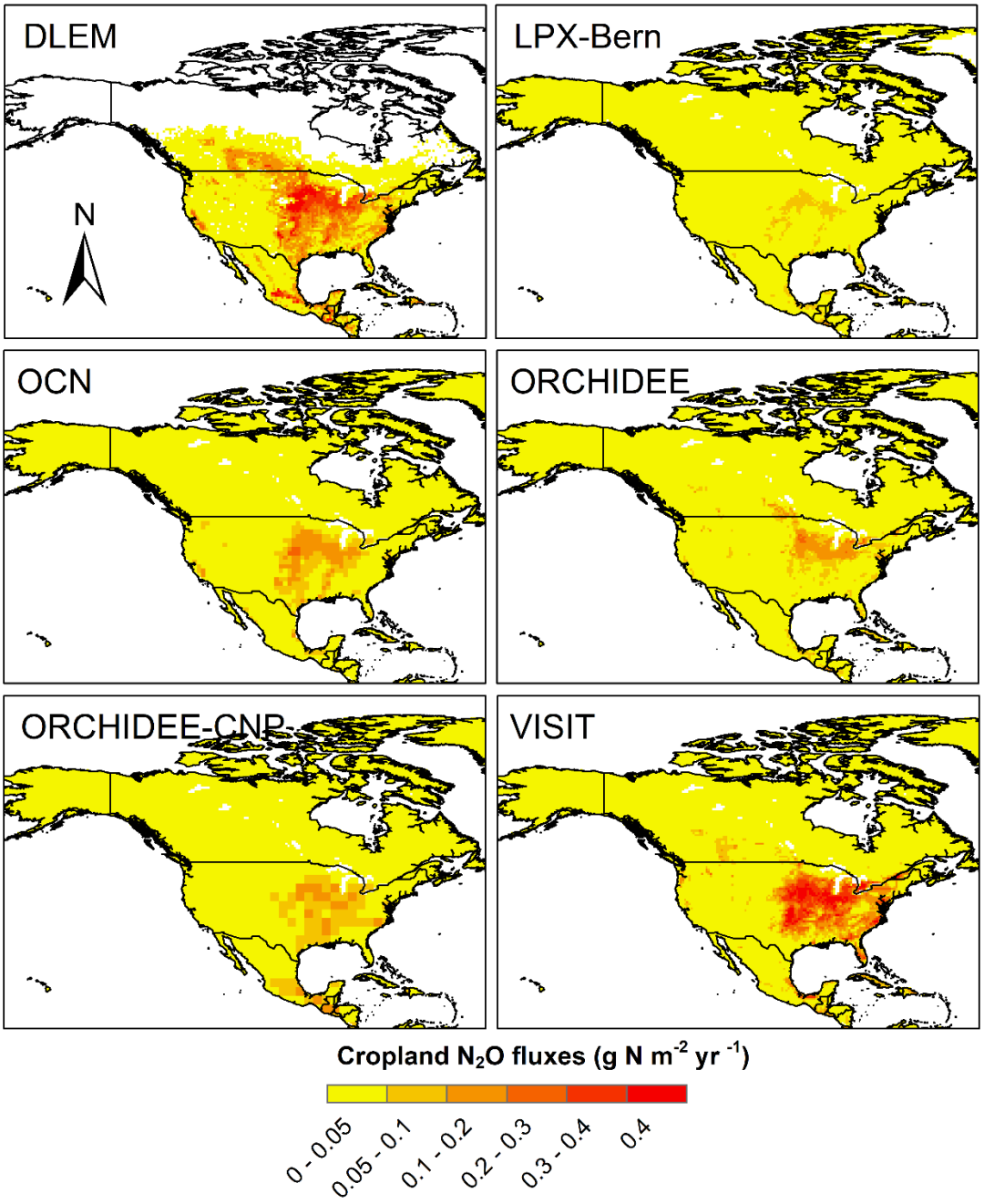

104

105 **Figure S7.** Spatial distribution of cropland N_2O emissions by BU approaches. Six terrestrial
106 biosphere models include DLEM, LPX-Bern, OCN, ORCHIDEE, ORCHIDEE-CNP, and VISIT.

107

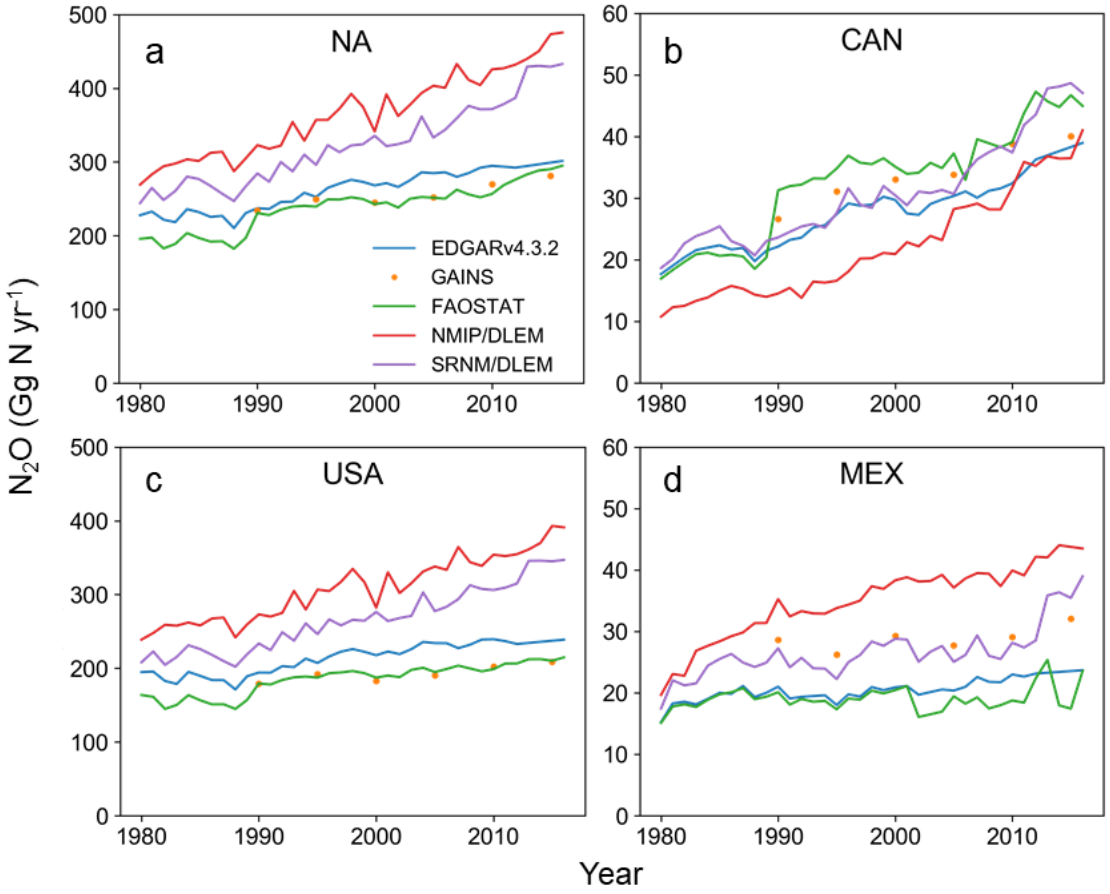

Figure S8. Direct emission from agricultural soils associated with mineral fertilizer, manure and crop residue inputs, and cultivation of organic soils based on EDGAR v4.3.2, GAINS, FAOSTAT, NMIP/DLEM, and SRNM/DLEM estimates in **(a)** North America, **(b)** Canada, **(c)** the U.S., and **(d)** Mexico.

Table S1. Decadal changes in anthropogenic N_2O sources over the past four decades over North America including the U.S., Canada, and Mexico.

		Decadal change (%)			
Anthropogenic sources		USA	Canada	Mexico	North America
Direct emissions of N additions in the agricultural sector (Agriculture)	Direct soil emissions	41	101	33	45
	Manure left on pasture	-7	30	7	-6
	Manure management	1	31	5	17
	Aquaculture	N/A	N/A	N/A	124
	sub-total	**27**	**80**	**18**	**29**
Other direct anthropogenic sources	Fossil fuel and industry	-26	-61	2283	1
	Waste and waste water	45	34	57	47
	Biomass burning				
	sub-total	**-22**	**-58**	**1168**	**3**
Indirect emissions from anthropoenic N additions	Inland waters, estuaries, coastal zones	12	10	1	10
	Atmospheric N deposition on land	-2	19	33	4
	sub-total	**3**	**13**	**20**	**6**
Perturbed fluxes from climate/CO2/land cover change	Climate & CO_2 effect	73	61	112	66
	Post-deforestation pulse effect	-3	-12	-14	-5
	Long-term effect of reduced mature forest area	-7	-1	19	0
	sub-total	**18**	**11**	**137**	**9**
Anthropogenic total		**7**	**-1**	**114**	**14**

Table S2. Information on North American N_2O measurement sites used in the global inversions from 1995 to 2016. CCG represents for discrete air samples from the National Oceanic and Atmospheric Administration Carbon Cycle Cooperative Global Air Sampling Network (NOAA); CSI represents for N2O measurements from the Commonwealth Scientific and Industrial Research Organization network (CSIRO); and AGA and CAT represent for N2O measurements from in-situ instruments in the Advanced Global Atmospheric Gases Experiment network (AGAGE) and the NOAA CATS network, respectively.

The global inversions: PyVAR-CAMS, INVICAT, GEOS-Chem				
Sites	**Latitude (°)**	**Longitude (°)**	**Altitude (m)**	**Type (FM: flask; CM: continuous)**
ALT_CCG	82.45	-62.52	205	FM
ALT_CSI	82.45	-62.52	210	FM
BAO_CCG	40.05	-105.01	1884	FM
BRW_CAT	71.32	-156.61	11	CM
BRW_CCG	71.32	-156.61	13	FM
CBA_CCG	55.21	-162.72	25	FM
ESP_CSI	49.38	-126.55	39	FM
HSU_CCG	41.05	-124.73	7.6	FM
KEY_CCG	25.67	-80.2	6	FM
KUM_CCG	19.52	-154.82	8	FM
LEF_CCG	45.93	-90.27	868	FM
LLB_CCG	54.95	-112.45	546	FM
MEX_CCG	18.98	-97.31	4469	FM
MID_CCG	28.22	-177.37	11	FM
MLO_CAT	19.54	-155.58	3397	CM
MLO_CCG	19.53	-155.58	3402	FM
MLO_CSI	19.53	-155.58	3397	FM
MVY_CCG	41.33	-70.51	12	FM
MWO_CCG	34.22	-118.06	1774	FM
NWR_CAT	40.05	-105.58	3526	CM
NWR_CCG	40.05	-105.58	3526	FM
PTA_CCG	38.95	-123.73	22	FM
SCT_CCG	33.41	-81.83	420	FM
SGP_CCG	36.62	-97.48	374	FM
SHM_CCG	52.72	174.1	28	FM
STR_CCG	37.75	-122.45	370	FM
THD_AGA	41.05	-124.15	107	CM
THD_CCG	41.05	-124.15	112	FM
UTA_CCG	39.9	-113.72	1332	FM
WBI_CCG	41.72	-91.35	621	FM
WGC_CCG	38.26	-121.49	483	FM
The global inversion: MIROC4-ACTM				
Sites	**Latitude (°)**	**Longitude (°)**	**Altitude (m)**	**Type (FM: flask)**
BRW_CCG	71.32	-156.61	11	FM
CBA_CCG	55.21	-162.72	21.34	FM
KUM_CCG	19.52	-154.82	3	FM
KEY_CCG	25.67	-80.16	1	FM
NWR_CCG	40.05	-105.59	3523	FM

Table S3. Information on North American N_2O measurement sites used in the CT-L regional inversion from 2007 to 2015 (Modified from Nevison et al., 2018).

Site	Latitude (°)	Longitude (°)	Altitude m agl (*asl)	Number of Measurements	Data Period
Surface Sites					
AMT	45.0	-68.7	107	1460	1/07-12/15
BAO	40.1	-105.0	300	2880	8/07-12/15
BMW	32.3	-64.9	30	341	1/07-12/15
BRW	71.3	-156.6	17	933	1/07-12/15
CBA	55.2	-162.7	36	656	1/07-12/15
CRV	65.0	-147.6	32	824	10/11-12/15
HSU	41.0	-124.3	8	72	5/08-12/15
INX	39.6 to 39.9	-86.4 to -85.7	156 to 225	1168	10/10-12/15
KEY	25.7	-80.2	5	394	1/07-12/15
LEF	45.9	-90.3	244 or 396	3138	1/07-12/15
LLB	55.0	-112.5	48	193	1/08-2/13
MBO	44.0	-121.7	11	629	10/11-5/14
MEX	19.0	-97.3	4469*	282	1/09-12/15
MLS	39.5 to 40.6	-110.2 to -104.5	0 to 13	289	6/08-7/08 and 6/11-6/12
MWO	34.2	-118.1	1774*	2040	4/10-12/15
NWR	40.0	-105.6	3526*	730	1/07-12/15
POC	10 to 35	-145 to -118	20	258	1/07-1/12
SCT	33.4	-81.8	305	1867	8/08-12/15
SGP	36.6	-97.5	60	452	1/07-12/15
STR	37.8	-122.5	486*	4036	10/07-12/15
THD	41.0	-124.2	5	453	1/07-12/15
UTA	39.9	-113.7	5	333	1/07-12/15
WBI	41.7	-91.4	379	2876	6/07-12/15
WGC	38.3 to 39.3	-121.5	91	2037	9/07-12/15
WKT	31.3	-97.3	5, 122 or 457	2427	1/07-12/15
Aircraft Sites					
ACG	57.0 to 76.6	-169.7 to -131.8	883 to 7969	1382	6/09-9/15
CAR	40.1 to 40.9	-105.2 to -104.1	665 to 6658	2246	1/07-12/15
CMA	38.4 to 39.0	-76.5 to -74.1	284 to 7422	1858	1/07-12/15
DND	47.2 to 48.5	-99.5 to -96.2	138 to 7002	1202	1/07-12/15
ESP	49.3 to 49.6	-126.6 to -125.7	314 to 5149	2432	1/07-12/15
ETL	53.9 to 54.6	-105.3 to -104.4	463 to 6165	2180	1/07-12/15
HIL	39.9 to 40.2	-88.1 to -87.7	727 to 7549	1642	1/07-12/15
LEF	45.7 to 46.1	-90.4 to -89.9	160 to 3250	2133	1/07-12/15
MLS	32.1 to 48.8	-112.2 to -96.1	2 to 3390	760	2/12-10/15
NHA	42.8 to 43.1	-70.7 to -70.3	321 to 7300	2241	1/07-12/15
PFA	64.1 to 65.9	-151.1 to -146.0	2343 to 6467	2342	1/07-12/15
SCA	32.5 to 33/9	-79.8 to -79.3	332 to 7861	1888	1/07-12/15
THD	40.9 to 41.6	-124.4 to -123.9	311 to 7901	1236	1/07-12/15
TGC	27.4 to 27.9	-97.0 to -96.5	317 to 7893	1434	1/07-12/15
WBI	41.6 to 42.5	-91.9 to -91.1	372 to 6372	1376	1/07-12/15

Table S4. Overview of the global and regional inversion frameworks.

	Name	Method	ACTM horizontal resolution	Ocean prior
Global inversion models	INVICAT	4D-Var	5.625°×5.625°	1 (high)
	PyVAR-CAMS-1	4D-Var	3.75°×1.875°	1 (high)
	PyVAR-CAMS-2			2 (low)
	MIROC4-ACTM	Bayesian analytical	2.8°×2.8°	3 (low)
	GEOS-Chem	4D-Var	5°×4°	2 (low)
Regional inversion model	CT-L	Bayesian analytical	1°×1°	NA

References

Beusen, A. H., Bouwman, A. F., Van Beek, L. P., Mogollón, J. M., & Middelburg, J. J. (2016). Global riverine N and P transport to ocean increased during the 20th century despite increased retention along the aquatic continuum. *Biogeosciences, 13*(8), 2441-2451.

Bouwman, A. F., Beusen, A., Overbeek, C., Bureau, D., Pawlowski, M., & Glibert, P. (2013). Hindcasts and future projections of global inland and coastal nitrogen and phosphorus loads due to finfish aquaculture. *Reviews in Fisheries Science, 21*(2), 112-156.

Bouwman, A. F., Pawłowski, M., Liu, C., Beusen, A. H., Shumway, S. E., Glibert, P., & Overbeek, C. (2011). Global hindcasts and future projections of coastal nitrogen and phosphorus loads due to shellfish and seaweed aquaculture. *Reviews in Fisheries Science, 19*(4), 331-357.

FAO, 2021. FAOSTAT Emissions database, http://www.fao.org/faostat/en/#data/GT, FAO, Rome, Italy.

Janssens-Maenhout, G., Crippa, M., Guizzardi, D., Muntean, M., Schaaf, E., Dentener, F., et al. (2019). EDGAR v4.3.2 Global Atlas of the three major greenhouse gas emissions for the period 1970–2012. *Earth System Science Data, 11*(3), 959-1002. https://www.earth-syst-sci-data.net/11/959/2019/

Lauerwald, R., Regnier, P., Figueiredo, V., Enrich-Prast, A., Bastviken, D., Lehner, B., et al. (2019). Natural lakes are a minor global source of N_2O to the atmosphere. *Global Biogeochemical Cycles, 33*, 1564-1581.

Maavara, T., Lauerwald, R., Laruelle, G. G., Akbarzadeh, Z., Bouskill, N. J., Van Cappellen, P., & Regnier, P. (2019). Nitrous oxide emissions from inland waters: Are IPCC estimates too high? *Global change biology, 25*(2), 473-488.

MacLeod, M., Hasan, M. R., Robb, D. H. F., & Mamun-Ur-Rashid, M. (2019). *Quantifying and mitigating greenhouse gas emissions from global aquaculture*. Retrieved from Rome.

Nevison, C., Andrews, A., Thoning, K., Dlugokencky, E., Sweeney, C., Miller, S., et al. (2018). Nitrous Oxide Emissions Estimated With the CarbonTracker-Lagrange North American Regional Inversion Framework. *Global Biogeochemical Cycles, 32*(3), 463-485.

Tian, H. Q., Yang, J., Xu, R. T., Lu, C. Q., Canadell, J. G., Davidson, E. A., et al. (2019). Global soil nitrous oxide emissions since the preindustrial era estimated by an ensemble of terrestrial biosphere models: Magnitude, attribution, and uncertainty. *Global change biology, 25*(2), 640-659. <Go to ISI>://WOS:000456028900021

Tubiello, F., Cóndor-Golec, R., Salvatore, M., Piersante, A., Federici, S., Ferrara, A., et al. (2015). *Estimating greenhouse gas emissions in agriculture: a manual to address data requirements for developing countries*. Retrieved from Rome

Van Der Werf, G. R., Randerson, J. T., Giglio, L., Van Leeuwen, T. T., Chen, Y., Rogers, B. M., et al. (2017). Global fire emissions estimates during 1997-2016. *Earth System Science Data, 9*, 697-720.

Wang, Q., Zhou, F., Shang, Z., Ciais, P., Winiwarter, W., Jackson, R. B., et al. (2019). Data-driven estimates of global nitrous oxide emissions from croplands. *National Science Review, 00*, 1-12.

Winiwarter, W., Höglund-Isaksson, L., Klimont, Z., Schöpp, W., & Amann, M. (2018). Technical opportunities to reduce global anthropogenic emissions of nitrous oxide. *Environmental Research Letters, 13*(1), 014011.

Yao, Y., Tian, H., Shi, H., Pan, S., Xu, R., Pan, N., & Canadell, J. G. (2020). Increased global nitrous oxide emissions from streams and rivers in the Anthropocene. *Natural Climate Change, 10*(2), 138-142.

180